Self-management of ROV umbilical using sliding buoys and stop

Christophe Viel

Self-management of ROV umbilical using sliding buoys and stop

Christophe Viel*

Abstract—The umbilical of Remote Operated Vehicle (ROV) has two main problems: it is subject to entanglement with obstacles or itself, and its shape is difficult to predict for the navigation. To address these issues, this article proposes a passive self-management of an ROV's umbilical, suitable for underwater and seafloor exploration. By adding two buoys moving freely on the umbilical, the described method avoids self-entanglement of the cable by stretching it, and gives it a predictable shape. A fast time computational model of the cable is proposed to provide feedback to the operator. The buoys move on their own to keep the cable taut without a motorized system, making this method easy to adapt to existing ROVs with few constraints on their navigation. Simulations and experimentation in pool show the effectiveness of the method. The influence of currents is discussed.

Keywords—Underwater robotics, cables management, cables model

I. Introduction

The Remotely Operated Vehicle (ROV) are submarine robots linked by underwater umbilicals to a control unit or a Human-Machine interface. This cable allows to transmit information in real time in both directions (see [5], [18]), to supply the robot with energy, to maintain a lifeline with the robot to avoid losing it [17]. However, umbilicals present several problems, such as collision with external objects, entanglement, inertia and drag forces impacting navigation, cable breakage, etc... which makes it a compromise between its constraint and its advantages [6].

Knowledge of the umbilical's shape has two main interests: to design the umbilical parameters to limit weight and entanglement problems, and to help the operator to prevent entanglement with an obstacle during the dive. To provide feedback on the position and shape of the umbilical, this one can be modeled, equipped or instrumented. Two main categories of methods can be observed in the literature: detection of the umbilical, using vision [14], [15], [16] and/or sensor placed directly on/in the umbilical [7], [10], and direct modeling of the umbilical using only the boat and ROV positions [11], [12], [9]. The main advantage of the first category is that an accurate model can be obtained in real time, but the equipment are often expensive and complex to install. In contrast, modeling strategies are cheap, but often less accurate and can not always provide real-time results.

Several methods exist to model the shape and dynamic of the cable, from the simplest geometrical model like catenary curve [19] or the chain of segments [11], to the finite-element methods [9]. Geometrical models are ideal for simulating a large number of segments in real-time and are memory efficient when an accurate physical model is not required. In opposite, the Lumped-mass-spring method [4], [12], [13] and the segmental methods [8], [9], [2] provide accurate results but with significant computational time. The first method models the umbilical as mass points joined together by massless elastic elements, the second describes the cable as a continuous system and numerically solves resulting partial differential equations.

The umbilical can also be equipped to better managed it. A TMS (Tether Management System), a underwater winch controlled by a human operator and attached to the ROV cage [1], can thus be used to regulate the amount of tether and thus keep the umbilical taut. However, this system is heavy for the cable, and operating it can be a complex task, so several works attempt to automate it or replace it with another vehicle such as a USV [20], a secondary ROV or multiple ROVs [16], or a motorized plug/float assembly [3]. The main inconvenient of these methods is that they must be managed automatically or by an operator in real time, which implies the necessity to know ROV's parameters that are sometime difficult to obtain.

This paper proposes passive self-management strategies of the umbilical of an ROV for underwater exploration using mobile buoys without motorization. Since the shape of the umbilical can be complex to predict when it can move freely, we propose to add sliding buoys, separated on the umbilical by stops, to stretch the cable and assimilate its shape to straight lines simple to model. This work extends previous work [21] by adding the concept of stop inside the cable and eliminating areas where umbilical could not be stretched. The main contributions are

- a passive self-management of the umbilical using sliding buoys and stops to stretch it without motorization nor TMS, allowing the ROV to evolve without risk of self-entanglement,
- a method simple to add to existing ROVs with a light and simple setup thanks to its passive attribute,
- an umbilical shape adapted to the sea and seafloor exploration with the presence of large obstacles,
- a model of the umbilical simple to compute in real time, helping the operator to prevent collisions with environmental obstacles.

*C Viel is with the CNRS, Lab-STICC, F-29806, Brest, France, inside the team Robex. email: christophe.viel@ensta-bretagne.fr

Manuscript received January 5, 2022.

In opposite with [3], the buoys are not motorized and move by themselves to keep the cable taut using only weight and Archimedes force. The umbilical is modeled using geometrical relations and the Fundamental Principle of Static (FPS) for a computationally faster and lighter approach than than lumped-mass-spring method or segmental methods studied in [4], [8], [9], [12].

The problematic and the hypotheses taken in this paper are described in Section II. The strategy of management of the umbilical is presented in Section III. The subsections III-A and III-C described its geometrical and dynamical model. Restricted areas guaranteeing the umbilical is always taut are described in Section III-E. The forces applied on the system are described in Section III-G. Finally, a choice of the parameters is proposed in Section III-H. The Section IV and V discuss of the validity of the previous models and hypotheses taken, based on experimentation. Finally, the Section VI concludes this work.

II. Problematic and hypothesis

Consider the referential $\mathcal{R}$ where the vertical axis is oriented to the ground such that $y = 0$ corresponds to the sea level and $y_1 > y_2$ means that y_1 is deeper than y_2. Let $O = (0, 0)$ and $R = (x, y)$ be the boat's and ROV's coordinates. The umbilical is attached between O and R.

In absence of tension, a cable will take on an irregular shape. To prevent the cable from moving freely and becoming entangled with itself or its environment, a technique mostly used for shallower dives is to hang a ballast at a fixed length on the umbilical to stretch it between the boat and the ballast. However, when the ROV is too close to the ballast, the cable between them takes the shape of a bell, subject to entanglement. In order to keep the umbilical taut independently of the robot's position, we proposes to equip the umbilical with others elements.

A ballast or a buoy tied to a cables, called "fixed", can usually only stretch one part of it, both in particular configuration. However, a ballast/buoy moving freely along the cable, called it "sliding", will always find its position at the lowest/highest point, corresponding to its minimum potential energy, where it stretches both parts of the cable simultaneously. Thus, an succession of sliding ballast and/or buoy on the umbilical is an interesting solution to stretch it. However, each sliding element must be restrained to a specific part of the cable with stops to prevent the elements from staying in contact at the same minimum potential energy. This paper proposes a configuration to stretch the umbilical using an anchor and two sliding buoys, without motorization nor TMS, simple to set up. The shape of the umbilical is so similar to predictable straight lines. The main advantage of using only sliding elements and not combination of sliding and fixed elements as in [21] is that it allows the umbilical to be stretched in all situations since the buoys don't reach the surface or ballasts touch the seafloor.

The following assumption are considered in all the study:

A1) The forces applied on the umbilical due to its mass/buoyancy are negligible compare to the action made by the sliding buoys and the anchor.

A2) The length of the umbilical is such that it is reasonable to neglect its length variation, considered as constant.

A3) When the umbilical is taut, its geometry can be assimilated to straight lines between defined points, here the buoys, the boat and the ROV. The rigidity of the cable can be modeled by a minimal angle $\theta_{\min}$ between the straight lines, described in [21].

A4) Consider the ROV, boat and anchor are strong enough to compensate action of the cables and buoys, and therefore remain stationary. (x, y) is so fixed when ROV is not moving.

A5) Let $F_{bi} = (\rho_{water} V_{b_i} - m_{b_i})\, g + F_{cy,b_i}$ be the force of the buoy b_i, with m_{b_i} its mass, V_{b_i} its volume, ρ_{water} the density of the water, and F_{cy,b_i} be the force exerted by the vertical current applied to the buoy's position such that $F_{cy,b_i} < 0$ pushes down to the seafloor and $F_{cy,b_i} > 0$ pushes up to the surface. It is assumed that the buoy's buoyancy is stronger than its weight and current forces, $i.e.$ $F_{b_i} > 0$.

A6) Consider the sliding buoys move freely on the umbilical without friction.

A7) The end of a cable connected to an anchor or to the boat is assumed to be perfectly fixed. A cable connected at both ends by the boat and the anchor does not need to meet the Assumption A1-A3.

A8) Consider absence of horizontal current in this study.

The validity of these hypotheses in practical cases will be discussed in Sections IV and V. To solve several systems in this paper, the following Theorem 1 is defined.

Theorem 1. *For the known parameters x, $l_a > 0$, $l_b > 0$, $\Lambda_{ab} > 0$, the solution of the system*

$$\begin{cases} x = l_a \sin(\theta_a) + l_b \sin(\theta_b) \\ \tan(\theta_b) = \Lambda_{ab} \tan(\theta_a). \end{cases} \tag{1}$$

can be expressed such

1) if $\Lambda_{ab} = 1$, one has $\theta_a = \theta_b$ and $\sin(\theta_a) = \frac{x}{(l_a + l_b)}$

2) if $\Lambda_{ab} \neq 1$, one has

$$\sin(\theta_a) = F(x, l_a, l_b, \Lambda_{ab}) \tag{2}$$

$$\theta_b = atan(\Lambda_{ab} \tan(\theta_a)) \tag{3}$$

where

$$F(x, l_a, l_b, \Lambda_{ab}) = \min_{i \in [1,2,3,4]} (|X_i|)\, sgn(x) \tag{4}$$

$$\begin{cases} X_1 = \frac{\sqrt{U - \frac{2}{3}A} - \sqrt{\Delta_{Y1}}}{2}, X_2 = \frac{\sqrt{U - \frac{2}{3}A} + \sqrt{\Delta_{Y1}}}{2} & \text{if } \Delta_{Y1} \geq 0 \\ X_1 = \infty, X_2 = \infty \quad \text{else,} \end{cases} \tag{5}$$

$$\begin{cases} X_3 = \frac{-\sqrt{U - \frac{2}{3}A} - \sqrt{\Delta_{Y2}}}{2}, X_4 = \frac{-\sqrt{U - \frac{2}{3}A} + \sqrt{\Delta_{Y2}}}{2} & \text{if } \Delta_{Y2} \geq 0 \\ X_3 = \infty, X_4 = \infty \quad \text{else,} \end{cases} \tag{6}$$

$$\text{for } \Delta_{Y1} = -\left(U + \tfrac{4}{3}A + \frac{2B}{\sqrt{U - \frac{2}{3}A}}\right) \text{ and } \Delta_{Y2} =$$

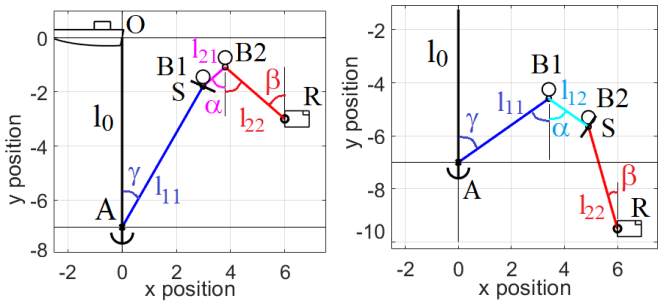

Fig. 1: Geometrical parameters. Right: $B1$ in contact with S. Left: $B2$ in contact with S. The black, blue, cyan, magenta, red lines correspond to l_0, l_{11}, l_{12}, l_{21}, l_{22}. Here, $F_{b2} = 2F_{b1}$.

$-\left(U + \frac{4}{3}A - \frac{2B}{\sqrt{U - \frac{2}{3}A}}\right)$ *with*

$$A = -\frac{x^2}{2l_a^2} - \frac{\left(l_b^2\Lambda_{ab}^2 - l_a^2\right)}{l_a^2\left(\Lambda_{ab}^2 - 1\right)} \tag{7}$$

$$B = -\frac{l_a^2 + l_b^2\Lambda_{ab}^2}{l_a^3\left(\Lambda_{ab}^2 - 1\right)}|x| \tag{8}$$

$$C = \frac{x^4}{16l_a^4} + \frac{x^2\left(l_a^2 - l_b^2\Lambda_{ab}^2\right)}{4l_a^4\left(\Lambda_{ab}^2 - 1\right)} \tag{9}$$

$$U = \begin{cases} \left(-\frac{q}{2} + \sqrt{\frac{q^2}{4} + \frac{p^3}{27}}\right)^{\frac{1}{3}} + \left(-\frac{q}{2} - \sqrt{\frac{q^2}{4} + \frac{p^3}{27}}\right)^{\frac{1}{3}} & \text{if } \Delta_U > 0, \\ 2\cos\left(\frac{1}{3}acos\left(-\frac{q}{2\sqrt{-\frac{p^3}{27}}}\right)\right)\sqrt{-\frac{p}{3}} & \text{if } \Delta_U < 0, \\ \sqrt{-\frac{p}{3}} & \text{if } \Delta_U = 0 \end{cases} \tag{10}$$

with $\Delta_U = \frac{q^2}{4} + \frac{p^3}{27}$, $p = -4C - \frac{A^2}{3}$ *and* $q = \frac{2A^3}{27} + \left(4AC - B^2\right) + \frac{-4CA}{3}$.

The proof of Theorem 1 is provided in Appendix A. Remark if several configurations must be considered in Theorem 1, a solution always exists and is analytic, so can be evaluated quickly.

III. Umbilical for seafloor and diving exploration

This section proposes a configuration adapted to the seafloor exploration, where the anchor is placed on the ground or few meters higher. The umbilical is taut by two buoys, keeping it far from the seafloor and so a potential obstacle.

A. Geometrical model and restricted areas

1) System description: The following parameters are illustrated in Figure 1. The umbilical of length l is divided into three parts: the first part $l_0 = \|OA\|$ between the boat O and an anchor A, the second part $l_1 = \|AS\|$ between the anchor A and the fixed stop S, and the last part $l_2 = \|SR\|$ between the stop S and the ROV R. A first buoy $B1$ can move freely on the cable l_1 between A and S, and a second buoy $B2$ can move freely on the cable l_2 between S and R. The length l_1 can be divided in two lengths $l_{11} = \|A\,B1\|$ and $l_{12} = \|B1\,S\|$ on each side of the buoy $B1$ with $l_1 = l_{11} + l_{12}$, and the length l_2 can also be divided in two lengths $l_{21} = \|S\,B2\|$ and $l_{22} = \|B2\,R\|$ on each side of $B2$ with $l_2 = l_{21} + l_{22}$.

Let γ be the oriented angle between the anchor and the buoy $B1$. The oriented angles α and β are respectively the angles between the buoys $B1$ and $B2$, and between the buoy $B2$ and the ROV. Let define F_{b1} and F_{b2} the force applied on the umbilical by the buoys $B1$ and $B2$, respecting assumption A5.

According to Assumption A7, l_0 is immobile and doesn't need to respect the Assumptions A1-A3: l_0 can thus takes all the cable deformation due to its length for a deep dive for example. Let's $(x_A, y_A) = (0, l_0)$ be the anchor's coordinate.

Note that a reverse model to this one, with ballasts instead of buoys, can be used to explore near the surface, see Figure 3.

B. Parameters constraints

Let define y_{floor} the minimum depth, *i.e.* the seafloor or a rock). Since the buoys $B1$ and $B2$ make the umbilical floating, the anchor is the lowest element and so l_0 must respect

$$l_0 \leq y_{\text{floor}} \tag{11}$$

where $l_0 = y_{\text{floor}}$ induce the anchor is placed on the seafloor.

The buoy $B1$ must not reach the surface for the cable l_1 to remain taut. Thus, l_0 and l_1 must be limited to

$$l_0 \geq l_1 + \max\left([h_{b1}, h_{b2}]\right) \tag{12}$$

where h_{b1} and h_{b2} are respectively the height of the submerged part of the buoy $B1$ and $B2$ when it floats freely on the surface. Finally, to ensure that it is possible to keep the cable stretched at $x = 0$, one must have

$$l_2 \leq l_0 - l_1 + y_{\text{floor}}. \tag{13}$$

1) Configuration areas: In function of the ROV position, the buoy $B1$ can be in contact with the stop S or the anchor A, and the buoy $B2$ with the stop S, the ROV or the surface. In some configuration, one buoy can move on its cable without being in contact with something, but since the two buoys try to raise to the surface, it is impossible to have the both in the same time: one buoy is always in contact with the stop. Six areas corresponding to specific umbilical configurations plus the inaccessible area can so be observed, illustrated in Figure 2. The existence and the position of some areas depend of the parameters l_0, l_1 and l_2, but also buoys' force F_{b1} and F_{b2}.

The following areas exist in all cases:

- Area A1: first main area for sea exploration. The buoy $B1$ is in contact with the stop S and the buoy $B2$ can move freely on cable l_2. One has $l_{11} = l_1$, $l_{12} = 0$, $l_{21} > 0$, $l_{22} > 0$.
- Area A2: second main area for seafloor exploration. The buoy $B1$ can move freely on cable l_1 and the buoy $B2$ is in contact with the stop S. One has $l_{11} \geq 0$, $l_{12} \geq 0$, $l_{21} = 0$, $l_{22} = l_2$.
- Area D1: the buoy $B1$ is in contact with the stop S and the buoy $B2$ is in contact with the ROV. One has $l_{11} = l_1$, $l_{12} = 0$, $l_{21} = l_2$, $l_{22} = 0$ and $\beta = 0$.

- Area D2: the buoys $B1$ and $B2$ are in contact with the stop S. One has $l_{11} = l_1$, $l_{12} = 0$, $l_{21} = 0$, $l_{22} = l_2$ and $\alpha = 0$.
- Area D3: the buoy $B1$ is in contact with the anchor A and the buoys is in contact with the stop S. One has $l_{11} = l_1$, $l_{12} = 0$, $l_{21} = 0$, $l_{22} = l_2$ and $\alpha = 0$.
- Area F: area inaccessible to the ROV due to the umbilical length.

If $l_0 - (l_1 + h_{b2}) < l_2$, the buoy $B2$ can reach the surface for some ROV position. Thus, the following areas exist:

- Area B: the buoy $B2$ is on the surface but the buoy $B1$ can still taut the cables l_1 and l_2, such $l_{21} > 0$, $l_{22} > 0$.
- Area C: the buoy $B2$ is on the surface and the buoy $B1$ can not taut the cable l_2. This configuration must be avoided by the ROV.

The umbilical is perfectly taut in all configurations except in area C: the ROV must not enter in this area to avoid the appearance of entanglement.The shape of the areas depends of different parameters, as it will be shown in Section III-E. However, only the areas C and F are required to control the ROV without risk of entanglement, others areas are required only to model the umbilical shape.

2) Main advantage and inconvenient of studying configuration : One observes this strategy can switch with two main configurations: the sea exploration in area A1, and the seafloor in area A2. As illustrated in Figure 2b, the area A2 is interesting to explore the seafloor because l_{22} can be kept the most vertical possible while the buoy $B1$ keeps the cables l_{11} and l_{12} far from the seafloor, avoiding collision between obstacles and the umbilical. The ROV can so dive between obstacle without risk. Note l_0 can be chosen such the anchor is on the ground or few meters higher, in function of the obstacles' size. To keep l_{22} the most vertical possible, it is recommended to take the buoy $B2$ stronger than $B1$ and l_2 shorter than l_1: as more described in Section III-H, an interesting configuration is to keep a ration $\frac{F_{b2}}{F_{b1}} = \frac{l_1}{l_2}$.

Disadvantage of this method are 1) it is not adapted to explore close to the surface of the sea, 2) the actions of the two buoys created more forces on the ROV. Remind a reverse model of this method, with ballasts instead of buoys, can be made to explore close to the surface, as illustrated in Figure 3. This configuration is interesting when the surface is hilly like for example in a harbor, under the ice or in underground caves.

3) Geometrical model: Since the ROV can not go higher than the sea level, the ROV can move inside the circle $\mathcal{C}(A, l_1 + l_2)$ of radium $l_1 + l_2$ and center A while $y > 0$, $i.e.$ the ROV stays inside the water. In a configuration where the umbilical is taut, $i.e.$ the ROV is not inside areas C or F, the system can be expressed such

$$x = l_{11}\sin(\gamma) - (l_{12} + l_{21})\sin(\alpha) + l_{22}\sin(\beta) \quad (14)$$

$$y = l_0 - l_{11}\cos(\gamma) + (l_{12} - l_{21})\cos(\alpha) + l_{22}\cos(\beta) \quad (15)$$

$$l_1 = l_{11} + l_{12} \quad (16)$$

$$l_2 = l_{21} + l_{22} \quad (17)$$

where l_1 and l_2 are fixed and known, $l_1 \geq l_{11} \geq 0$, $l_1 \geq l_{12} \geq 0$, $l_2 \geq l_{21} \geq 0$ and $l_2 \geq l_{22} \geq 0$.

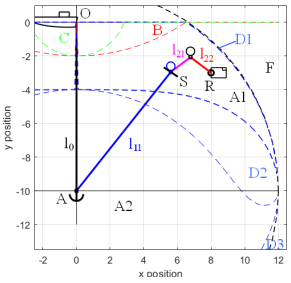

(a) Case $l_0 < l_2 + l_1 + h_{b2}$, $l_1 = 3l_2$ and $F_{b2} = 3F_{b1}$. Area A1: buoy $B1$ is in contact with the stop, $i.e.$ $l_{11} = l_1$, $l_{12} = 0$.

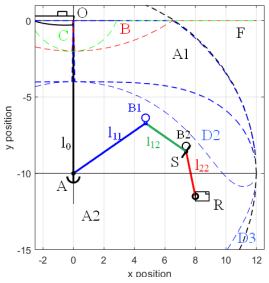

(b) Case $l_0 < l_2 + l_1 + h_{b2}$, $l_1 = 3l_2$ and $F_{b2} = 3F_{b1}$. Area A2: buoy $B2$ is in contact with the stop, $i.e.$ $l_{21} = 0$, $l_{22} = l_2$.

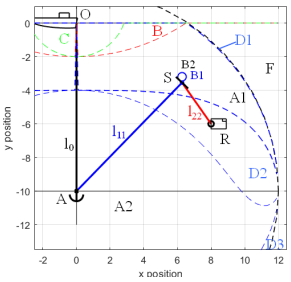

(c) Case $l_0 < l_2 + l_1 + h_{b2}$, $l_1 = 3l_2$ and $F_{b2} = 3F_{b1}$. Area D2: buoy $B1$ and $B2$ are in contact with the stop, $i.e.$ $l_{11} = l_1$, $l_{12} = 0$, $l_{21} = 0$, $l_{22} = l_2$.

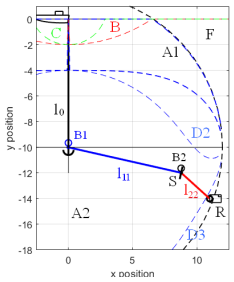

(d) Case $l_0 < l_2 + l_1 + h_{b2}$, $l_1 = 3l_2$ and $F_{b2} = 3F_{b1}$. Area D3: buoy $B1$ is in contact with the anchor and $B2$ with the stop, $i.e.$ $l_{11} = 0$, $l_{12} = l_1$, $l_{21} = 0$, $l_{22} = l_2$.

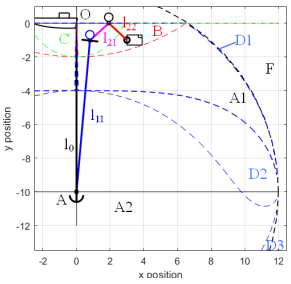

(e) Case $l_0 < l_2 + l_1 + h_{b2}$, $l_1 = 3l_2$ and $F_{b2} = 3F_{b1}$. Area B: buoy $B1$ is in contact with the stop and $B2$ with the surface, $i.e.$ $l_{11} = 0$, $l_{12} = l_1$.

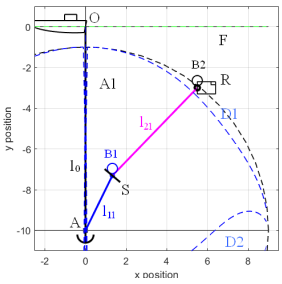

(f) Case $l_0 > l_2 + l_1 + h_{b2}$, $l_2 = 2l_1$ and $F_{b1} = 2F_{b2}$. Area D1: buoy $B1$ is in contact with the stop and $B2$ with the ROV, $i.e.$ $l_{11} = l_1$, $l_{12} = 0$, $l_{21} = l_2$, $l_{22} = 0$.

Fig. 2: Parameters for diving exploration. A is the anchor, M is the fixed ballast and B the sliding buoys. The black, blue, green, magenta, red lines correspond to l_0, l_{11}, l_{12}, l_{21}, l_{22}. Black dash line: area where the ROV can move with its umbilical length. Remark the position of area D2 changes with umbilical parameters, and areas B and C don't exist when $l_0 > l_2 + l_1 + h_{b2}$.

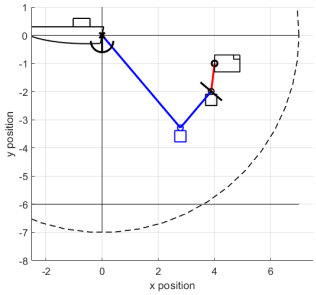

Fig. 3: Reversed model using sliding ballast instead of buoys

Since the buoy $B2$ is not in contact with the stop or the ROV, *i.e.* inside the area A1 or B, its position is on the ellipse $\mathcal{E}_1$ of centers $B1$ and R with the two radius $\frac{l_2}{2}$ and $\sqrt{\left(\frac{l_2}{2}\right)^2 - \frac{(x-x_{B1})^2+(y-y_{B1})^2}{4}}$, where (x_{B1}, y_{B1}) are the buoy's $B1$ coordinates. In absence of horizontal current, the ellipse properties show that

$$\alpha = -\beta \quad \text{if } (x,y) \in \text{area A1 or B.} \tag{18}$$

Else, $\beta \neq \alpha$ and one has $\alpha = 0$ if the buoy $B2$ is in contact with the stop, and $\beta = 0$ if the buoy $B2$ is in contact with the ROV.

In the same way, since the buoy $B1$ is not in contact with the stop or the anchor, *i.e.* inside the area A2, its position is on the ellipse $\mathcal{E}_2$ of centers $B2$ and A with the two radius $\frac{l_1}{2}$ and $\sqrt{\left(\frac{l_1}{2}\right)^2 - \frac{(x_A-x_{B2})^2+(y_A-y_{B2})^2}{4}}$, where (x_{B2}, y_{B2}) are the buoy's $B2$ coordinates. In absence of horizontal current, the ellipse properties show that

$$\alpha = -\gamma \quad \text{if } (x,y) \in \text{area A2.} \tag{19}$$

Else, $\gamma \neq \alpha$ and one has $\gamma = 0$ if the buoy $B1$ is in contact with the anchor.

Since (x, y) are known, the system (14)-(16) has 7 unknown parameters. From Section III-B1 and relations (18) and (19), many parameters of the system (14)-(16) can be simplified in function of the area where the ROV is located. These simplifications are enough to solve the system in all areas except in areas A1 and A2 where a last equation is missing. This missing equation can be found by studying the dynamic of the system, as exposed in next Section III-C.

C. Dynamic model in areas A1 and A2

In this section, cases where the ROV is inside the area A1 or A2 are studied to solve the system (14)-(15). Results exposed in this section are only valid in respectively areas A1 or A2. Others areas will be studied in next sections.

The dynamic of the system is studied at its equilibrium. Neither buoy touches the surface. Considering Assumption A1, let perform the FPS on $B1$ and $B2$, as illustrated in Figure 4:

$$\Sigma_{B1}\vec{F} = -F_{b1}\vec{y} + \vec{T_1} + \vec{T_2} \tag{20}$$

$$\Sigma_{B2}\vec{F} = -F_{b2}\vec{y} - \vec{T_3} - \vec{T_2} \tag{21}$$

where $\vec{T_1}$, $\vec{T_2}$ and $\vec{T_3}$ are the tension of the umbilical applied on the buoys.

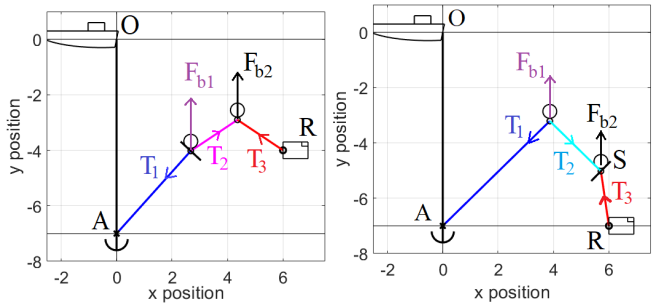

(a) Area A1 with $l_1 = l_2$ (b) Area A2 with $l_1 = 4l_2$

Fig. 4: Forces applied in areas A1 and A2. Here, $F_{b2} = 3F_{b1}$. The black, blue, green, magenta, red lines correspond to l_0, l_{11}, l_{12}, l_{21}, l_{22}. Black dash line: boundary with area F.

Studied of FPS in area A1: Consider first the area A1, as illustrated in Figure 4 a. The buoy $B1$ is in contact with the stop and the buoy $B2$ can move freely on l_2, so one has (18). Following steps described in Appendix C, one can show that

$$\tan(\beta) = \Lambda_{A1}\tan(\gamma) \quad \text{if } (x,y) \in \text{area A1} \tag{22}$$

where $\Lambda_{A1} = 2\frac{F_{b1}}{F_{b2}} + 1$ and remark $\Lambda_{A1} > 1$.

Studied of FPS in area A2: Consider now the area A2, as illustrated in Figure 4 b. The buoy $B2$ is in contact with the stop and the buoy $B1$ can move freely on l_1, so one has (19). Following steps described in Appendix D, one can show that

$$\tan(\beta) = \Lambda_{A2}\tan(\gamma) \quad \text{if } (x,y) \in \text{area A2} \tag{23}$$

where $\Lambda_{A2} = \frac{1}{2\frac{F_{b2}}{F_{b1}}+1}$ and remark $1 > \Lambda_{A2} > 0$.

D. Umbilical model solved in area A1 and A2

In this section, let's consider the ROV is inside the area A1 or A2. The Theorem 2 and 3 describes the value of parameters γ, α, β, l_{11}, l_{12}, l_{21} and l_{22}. For this section and the following ones, let not γ_{A1} and γ_{A2} the evaluations of γ inside the area A1 and A2, as described in the following theorems.

Theorem 2. *Consider the system* (14)-(15) *with* $(x,y) \in [-(l_1+l_2),(l_1+l_2)] \times [\max([0, l_0-(l_1+l_2)]), l]$ *and where* (x,y) *is inside the area A1, i.e.* $l_{11} = l_1$, $l_{12} = 0$, $l_{21} > 0$, $l_{22} > 0$. *Considering also the absence of horizontal current, i.e.* (18) *and* (22) *are true. The angle* γ *can be expressed as* $\gamma = \gamma_{A1}$ *such*

a) if $x = 0$, *the only geometrical solution is* $\gamma_{A1} = 0$,

b) else, γ_{A1} *can be expressed such*

$$\sin(\gamma_{A1}) = F(x, l_1, l_2, \Lambda_{A1}) \tag{24}$$

where $F(x, l_1, l_2, \Lambda_{A1})$ *is solution exposed in Theorem 1.*

The other parameters can be expressed such

$$\beta = atan(\Lambda_{A1}\tan(\gamma_{A1})) \tag{25}$$

$$l_{21} = \frac{l_2}{2} - \frac{y - l_0 + l_1\cos(\gamma_{A1})}{2\cos(\beta)} \tag{26}$$

and $l_{22} = l_2 - l_{21}$, $\alpha = -\beta$.

The proofs of Theorem 2 are described in Appendix E and F.

Theorem 3. *Consider the system* (14)-(15) *with* $(x,y) \in [-(l_1+l_2),(l_1+l_2)] \times [\max([0, l_0-(l_1+l_2)]), l]$ *and where* (x,y) *is inside the area A2, i.e.* $l_{11}>0$, $l_{12}>0$, $l_{21}=0$, $l_{22}=l_2$. *Considering also the absence of horizontal current, i.e.* (19) *and* (23) *are true. The angle* γ *can be expressed* $\gamma=\gamma_{A2}$ *such*

a) if $x=0$, *the only geometrical solution is* $\gamma_{A2}=0$,

b) else, γ_{A2} *can be expressed such*

$$\sin(\gamma_{A2}) = F(x, l_1, l_2, \Lambda_{A2}) \tag{27}$$

where $F(x,l_1,l_2,\Lambda_{A2})$ *is solution exposed in Theorem 1.*

The other parameters can be expressed such

$$\beta = atan(\Lambda_{A2}\tan(\gamma_{A2})) \tag{28}$$

$$l_{11} = \frac{l_1}{2} + \frac{l_0 - y + l_2\cos(\beta)}{2\cos(\gamma_{A2})} \tag{29}$$

and $l_{12}=l_1-l_{11}$, $\alpha=-\gamma_{A2}$.

The proofs of Theorem 3 are described in Appendix G and H.

Theorem 2 and 3 propose analytic solutions which always exists and the solution is analytic.

E. Boundaries of the areas

This section presents the different boundaries, where the areas A1 and A2 are defined as the default configurations. The calculation of these boundaries is described in Appendix I.

The boundary $y_{area\,B}(x)$ between the areas A1 and B correspond to the depth where the buoy is in contact with the surface, so $y = l_{22}\cos(\beta)+h_{b2}$ with $l_{22}\geq 0$. The area B does not exist if $l_2 < l_0-(l_1+h_{b2})$ because the buoy $B2$ can not reach the surface without come in contact with the ROV (area D1). Following steps from Appendix I1, $y_{area\,B}(x)$ can be expressed as

$$y_{area\,B}(x) = \begin{cases} 0 & \text{if } l_2 < l_0-(l_1+h_{b2}) \\ \max\left(\left[\frac{l_2+l_1\sqrt{1+\left(\Lambda_{A1}^2-1\right)\sin(\gamma_{A1}(x))^2}}{\sqrt{1+\Lambda_{A1}^2\tan(\gamma_{A1}(x))^2}}\right.\right. & \\ \left.\left. -l_0+2h_{b2}, h_{b2}\right]\right) & \text{else.} \end{cases} \tag{30}$$

Inside the area C, the buoy $B2$ is on the surface and the cable l_1 is vertical ($\gamma=0$), so the buoy $B1$ can not taut the cable l_2. Following steps from Appendix I2, the boundary $y_{area\,C}(x)$ between the areas C and B can be expressed as

$$y_{area\,C}(x) = \begin{cases} \max\left(\left[\sqrt{l_2^2-x^2}+l_1\right.\right. & \\ \left.\left. -l_0+2h_{b2}, h_{b2}\right]\right) & \text{if } (x\leq l_2)\,\&\,(l_2 > l_0-(l_1+h_{b2})) \\ h_{b2} & \text{if } (x>l_2)\,\&\,(l_2>l_0-(l_1+h_{b2})) \\ 0 & \text{else.} \end{cases} \tag{31}$$

Inside the area D1, the buoy $B2$ is in contact with the ROV and the buoy $B1$ in contact with the stop: one has $l_{11}=l_1$, $l_{12}=0$, $l_{22}=0$ and $l_{21}=l_2$. Following steps from Appendix I3, the boundary $y_{area\,D1}(x)$ between areas D1 and A1 can be expressed as

$$y_{area\,D1}(x) = \max\left(\left[l_0 - \frac{l_1\sqrt{1+(\Lambda_{A1}^2-1)\sin(\gamma_{A1}(x))^2}+l_2}{\sqrt{1+\Lambda_{A1}^2\tan(\gamma_{A1}(x))^2}}, 0\right]\right). \tag{32}$$

Inside the area D2, the buoys $B1$ and $B2$ are in contact with the stop, so $l_{11}=l_1$, $l_{12}=0$ $l_{22}=l_2$ and $l_{21}=0$. The ROV can enter inside the area D2 from area A1 or area A2: two boundaries must so be defined. Following steps from Appendices I4 and I5, the ROV is inside the area D2 if $y_{area\,A1-D2}(x) \leq y \leq y_{area\,A2-D2}(x)$ such

$$y_{area\,A1-D2}(x) = \max\left(\left[l_0 + \frac{-l_1\sqrt{1+(\Lambda_{A1}^2-1)\sin(\gamma_{A1}(x))^2}+l_2}{\sqrt{1+\Lambda_{A1}^2\tan(\gamma_{A1}(x))^2}}, 0\right]\right) \tag{33}$$

and

$$y_{area\,A2-D2}(x) = \max\left(\left[l_0 + \frac{-l_1\sqrt{1+(\Lambda_{A2}^2-1)\sin(\gamma_{A2}(x))^2}+l_2}{\sqrt{1+\Lambda_{A2}^2\tan(\gamma_{A2}(x))^2}}, 0\right]\right). \tag{34}$$

Inside the area D3, the buoy $B1$ is in contact with the anchor and the buoy $B2$ with the stop: one has $l_{11}=0$, $l_{12}=l_1$, $l_{22}=l_2$ and $l_{21}=0$. Following steps from Appendix I6, the boundary $y_{area\,D3}(x)$ between area D3 and A2 can be expressed as

$$y_{area\,D3}(x) = \max\left(\left[l_0 + \frac{l_1\sqrt{1+(\Lambda_{A2}^2-1)\sin(\gamma_{A2}(x))^2}+l_2}{\sqrt{1+\Lambda_{A2}^2\tan(\gamma_{A2}(x))^2}}, 0\right]\right). \tag{35}$$

Finally, since the area F corresponds to the limit of the umbilical length. Following steps from Appendix I7, the ROV is not inside the area F if $y_{area\,F1}(x) \leq y \leq y_{area\,F2}(x)$ where

$$y_{area\,F1}(x) = \max\left(l_0 - \sqrt{(l_1+l_2)^2-x^2},\, 0\right), \tag{36}$$

$$y_{area\,F2}(x) = l_0 + \sqrt{(l_1+l_2)^2-x^2}. \tag{37}$$

The limits $y_{area\,B}(x)$ and $y_{area\,C}(x)$ between areas B and C described above take into account the geometries of the buoy $B2$ which, in practice, hang above the umbilical (in Figure 2, one has $h_{b2}=0$. Note if $h_{b2}>0$, areas B and C are only lower of h_{b2}). Above the limit $y=h_{b2}$, the buoy floats freely and can not provide enough tension in the cable to predict the shape of this one.

One observes that the area B converges to area C when the ratio $\frac{F_{b1}}{F_{b2}}$ increases, while the area C changes with the discrepancy between l_0, l_1 and l_2. Note both does not exist if $l_2 \leq l_0 - (l_1 + h_{b2})$. Remark also the areas C and F depend only of l_0, l_1, l_2 and x, so can be easily modeled.

F. Umbilical model solved for all areas

As exposed in Section III-E, the different areas must be considered because they represent particular geometrical configurations.

For $y \neq l_0$, let define the parameters

$$X_{1D} = \frac{a_D b_D - \sqrt{a_D^2 b_D^2 - (1+b_D^2)(a_D^2-1)}}{(1+b_D^2)} \tag{38}$$

$$X_{2D} = \frac{a_D b_D + \sqrt{a_D^2 b_D^2 - (1+b_D^2)(a_D^2-1)}}{(1+b_D^2)} \tag{39}$$

with $a_D = \frac{x^2+(l_0-y)^2+l_1^2-l_2^2}{2(y-l_0)l_1}$ and $b_D = \frac{x}{y-l_0}$. In the same way, let define for $y > 0$ the parameters

$$X_{1B} = \frac{a_B b_B - \sqrt{a_B^2 b_B^2 - (1+b_B^2)(a_B^2-1)}}{(1+b_B^2)} \tag{40}$$

$$X_{2B} = \frac{a_B b_B + \sqrt{a_B^2 b_B^2 - (1+b_B^2)(a_B^2-1)}}{(1+b_B^2)} \tag{41}$$

where $a_B = \frac{x^2+(l_0+y-2h_{b2})^2+l_1^2-l_2^2}{2(l_0+y-2h_{b2})l_1}$ and $b_B = \frac{x}{l_0+y-2h_{b2}}$. Let's also define the conditions

$$T_{1B} = \left(a_B - b_B X_{1B} == \sqrt{1-X_{1B}^2}\right) \tag{42}$$

$$T_{2B} = \left(a_B - b_B X_{2B} == \sqrt{1-X_{2B}^2}\right) \tag{43}$$

$$T_{1D} = \left(a_D - b_D X_{1D} == -\sqrt{1-X_{1D}^2}\right) \tag{44}$$

$$T_{2D} = \left(a_D - b_D X_{2D} == -\sqrt{1-X_{2D}^2}\right) \tag{45}$$

$$T_{3D} = \left(a_D - b_D X_{1D} == \sqrt{1-X_{1D}^2}\right) \tag{46}$$

$$T_{4D} = \left(a_D - b_D X_{2D} == \sqrt{1-X_{2D}^2}\right). \tag{47}$$

The following Theorem 4 exposes the evaluation of the parameters γ, α, β, l_{11}, l_{12}, l_{21} and l_{22} in function of the area where the ROV is located.

Theorem 4. *Consider the system* (14)-(15) *for* $(x,y) \in [-(l_1+l_2),(l_1+l_2)] \times [\max([0, l_0-(l_1+l_2)]), l]$ *and* $y_{area\,F1}(x) < y < y_{area\,F2}(x)$. *Considering the absence of horizontal current, one gets*

(1) if $y < y_{area\,C}(x)$, *the ROV is inside area C: the model is not valid and the system* (14)-(15) *cannot be solved.*

(2) else if $y > 0$, $y_{area\,B}(x) \neq 0$ *and* $y_{area\,C}(x) \leq y \leq y_{area\,B}(x)$, *then* (x,y) *is in the area B and one has* $l_{11} = l_1$, $l_{12} = 0$, $l_{21} = l_2 - l_{22}$, $\beta = -\alpha$ *and*

$$\sin(\gamma_B) = \begin{cases} X_{1B} & \text{if } (T_{1B} == True)\,\&\,(T_{2B} == False) \\ X_{2B} & \text{if } (T_{1B} == False)\,\&\,(T_{2B} == True) \\ \min([X_{1B}, X_{2B}]) & \text{if } (T_{1B} == True)\,\&\,(T_{2B} == True) \end{cases} \tag{48}$$

$$l_{22} = \frac{l_2(y-h_{b2})}{l_0 - l_1\cos(\gamma_B) + (y-2h_{b2})} \tag{49}$$

$$\beta = sgn(x)\, acos\left(\frac{(y-2h_{b2}) + l_0 - l_1\cos(\gamma_B)}{l_2}\right). \tag{50}$$

(3) else if $y = 0$ *or* $y \leq y_{area\,D1}(x)$, *then* (x,y) *is in the area D1 and one has* $l_{11} = l_1$, $l_{12} = 0$, $l_{21} = l_2$, $l_{22} = 0$, $\beta = 0$, $\gamma = \gamma_{D1}$ *with*

$$\sin(\gamma_{D1}) = \begin{cases} \frac{x^2+l_1^2-l_2^2}{2l_1x} & \text{if } y = l_0 \\ X_{1D} & \text{if } (T_{1D} == True)\,\&\,(T_{2D} == False) \\ X_{2D} & \text{if } (T_{1D} == False)\,\&\,(T_{2D} == True) \\ \min([X_{1D}, X_{2D}]) & \text{if } (T_{1D} == True)\,\&\,(T_{2D} == True) \end{cases} \tag{51}$$

$$\alpha = -sgn(x)\, acos\left(\frac{-y + l_0 - l_1\cos(\gamma_{D1})}{l_2}\right). \tag{52}$$

(4) else if $y_{area\,A1-D2}(x) \leq y \leq y_{area\,A2-D2}(x)$, *then* (x,y) *is in the area D2 and one has* $l_{11} = l_1$, $l_{12} = 0$, $l_{21} = 0$, $l_{22} = l_2$, $\alpha = 0$,

$$\sin(\gamma_{D2}) = \begin{cases} \frac{x^2+l_1^2-l_2^2}{2l_1x} & \text{if } y = l_0 \\ X_{1D} & \text{if } (T_{1D} == True)\,\&\,(T_{2D} == False) \\ X_{2D} & \text{if } (T_{1D} == False)\,\&\,(T_{2D} == True) \\ \min([X_{1D}, X_{2D}]) & \text{if } (T_{1D} == True)\,\&\,(T_{2D} == True) \end{cases} \tag{53}$$

$$\beta = sgn(x)\, acos\left(\frac{y - l_0 + l_1\cos(\gamma_{D2})}{l_2}\right). \tag{54}$$

(5) else if $y_{area\,D3}(x) \leq y$, *then* (x,y) *is in the area D3 and one has* $l_{11} = 0$, $l_{12} = l_1$, $l_{21} = 0$, $l_{22} = l_2$, $\gamma = 0$, $\alpha = \alpha_{D3}$ *such*

$$\sin(-\alpha_{D3}) = \begin{cases} X_{1D} & \text{if } (T_{3D} == True)\,\&\,(T_{4D} == False) \\ X_{2D} & \text{if } (T_{3D} == False)\,\&\,(T_{4D} == True) \\ \min([X_{1D}, X_{2D}]) & \text{if } (T_{3D} == True)\,\&\,(T_{4D} == True) \end{cases} \tag{55}$$

$$\beta = sgn(x)\, acos\left(\frac{y - l_0 - l_1\cos(\alpha)}{l_2}\right). \tag{56}$$

(6) else if $y_{area\,A2-D2}(x) \leq y \leq y_{area\,D3}(x)$, *then* (x,y) *is in the area A2, one has the parameters defined in Theorem 3 such* $\gamma = \gamma_{A2}(x)$, $\alpha = -\gamma$, $l_{12} = l_1 - l_{11}$, $l_{21} = 0$ $l_{22} = l_2$ *with* $\tan(\beta) = \Lambda_{A2}\tan(\gamma_{A2})$ *and* $l_{11} = \frac{l_1}{2} + \frac{l_0 - y + l_2\cos(\beta)}{2\cos(\gamma_{A2})}$.

(7) else, then (x,y) *is in the area A1 and one has the parameters defined in Theorem 2 such* $\gamma = \gamma_{A1}(x)$, $\alpha = -\beta$, $l_{11} = l_1$, $l_{12} = 0$, $l_{22} = l_2 - l_{21}$ *with* $\tan(\beta) = \Lambda_{A1}\tan(\gamma_{A1})$ *and* $l_{21} = \frac{l_2}{2} - \frac{y - l_0 + l_1\cos(\gamma_{A1})}{2\cos(\beta)}$.

The proofs of previous results are described in Appendix J. Note if Theorem 4 (1) is true, the ROV must dive to $y = y_{area\,C}(x)$ to make the system valid.

G. Forces applied on the ROV

To choose the buoys in the capabilities of the ROV, this section exposes the force $\vec{F}_{cable\to ROV}$ applied by the umbilical on the ROV. These ones depend of buoy choices, but also of the umbilical configuration, thus the area where the ROV is.

1) forces applied in areas A1 and B: Following steps described in Appendix K1, $F_{cable\to ROV}$ can be expressed in areas A1 and B such

$$F_{cable\to ROV} = \frac{F_{b2}}{2\cos(\beta)}. \tag{57}$$

Deduce from (57) and Theorem 4 that $F_{cable\to ROV}$ increases with the distance $d = \sqrt{x^2+y^2}$. Since β is independent of y in area A1, one deduces that $F_{cable\to ROV}$ increases only with x in area A1.

2) forces applied in areas A2: Following steps described in Appendix K2, $F_{cable\to ROV}$ can be expressed in area A2 such

$$F_{cable\to ROV} = \frac{1}{\cos(\beta)}\left(F_{b2} + \frac{F_{b1}}{2}\right). \tag{58}$$

Similarly that for area A1, it can be deduced from (57) and Theorem 4 that $F_{cable\to ROV}$ increases only with x in area A2.

3) forces in area D1: Following steps described in Appendix K3, $F_{cable\to ROV}$ can be expressed in area D1 such

$$F_{cable\to ROV} = \sqrt{F_1^2\left(\frac{\sin(\gamma)}{\sin(\gamma-\alpha)}\right)^2 + F_{b2}^2 - 2\cos(\alpha)\left(\frac{\sin(\gamma)}{\sin(\gamma-\alpha)}\right)F_{b1}F_{b2}}. \tag{59}$$

Since $|\alpha| \in \left[0, \frac{\pi}{2}\right]$ inside the area D1, one deduces from (59) than $F_{cable\to ROV} \in \left[F_{b2}, \sqrt{F_{b1}^2+F_b^2}\right]$ inside the area D1, depending of α. One observes that $F_{cable\to ROV} = F_{b2}$ when $x = 0$,a coherent result because $\gamma = 0$, thus l_1 is vertical with the buoy $B1$ in contact with the stop S, so the action of $B1$ is completely balanced by the anchor and doesn't have influence on the cable l_2 or the ROV. Like in area A1, one can observe $|\alpha|$ increases only when $|x|$ increases in area D1, and so $F_{cable\to ROV}$.

4) forces in area D2: Following steps described in Appendix K4, $F_{cable\to ROV}$ can be expressed in area D2 such

$$F_{cable\to ROV} = \frac{(F_{b1}+F_{b2})}{\cos(\beta)} \tag{60}$$

where $\beta \in \left]0, \frac{\pi}{2}\right[$ in area D2. One observes that the force applied on the ROV is strong when the cable is close to the horizontal axis, *i.e.* (x, y) close to (l_1+l_2, l_0) and weaker close to vertical axis, *i.e.* (x, y) close to $(0, l_0)$.

5) forces in area D3: Following steps described in Appendix K5, $F_{cable\to ROV}$ can be expressed in area D3 such

$$F_{cable\to ROV} = \frac{F_{b2}}{\left(\frac{\sin(\beta)}{\tan(-\alpha)} - \cos(\beta)\right)}. \tag{61}$$

Remark $F_{cable\to ROV} = F_{b2}$ when $x = 0$ so $\beta = 0$ and $\alpha = \pi$, a coherent result because the cable l_2 is vertical when $\beta = 0$ and so buoy $B2$ lifts directly the ROV.

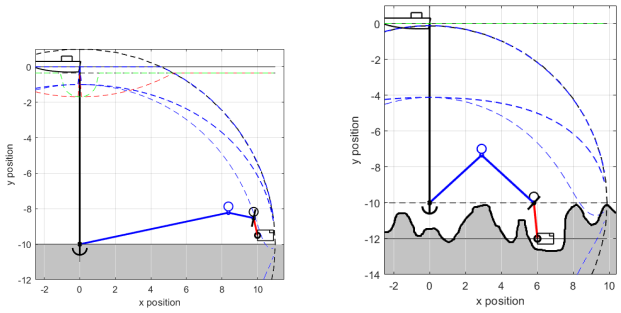

(a) without obstacles, $l_0 = y_{\text{floor}}$, $l_1 = 10l_2$, $F_{b2} = 10F_{b1}$

(b) with obstacles, $l_0 = y_{\text{floor}} - l_2$, $l_1 = 7.5l_2$, $F_{b2} = 5F_{b1}$, $\beta_{\max} = 10°$

Fig. 5: Choice of parameters for seafloor exploration.

H. Practical case: choice of umbilical length

This section proposes simple methods to choose the parameters l_0, l_1 and l_2 in function of several environmental constraints. Note these methods are suggestions and others values can be chosen.

Let's define $[y_{\min}, y_{\max}]$ the desired minimum depth and maximum depths for the ROV exploration, where $y_{\min} \geq h_B$ and $y_{\max} \leq y_{\text{floor}}$. Let's also define $[-x_{\max}, x_{\max}]$ the desired horizontal area with $x_{\max}$ the desired maximum horizontal distance for the ROV exploration. Compromises must be made because not all the parameters $x_{\max}$, $y_{\min}$, $y_{\max}$ will be respected simultaneously. In this perspective, since the boat can move on the surface, the respect of parameters $[y_{\min}, y_{\max}]$ is favored over $[x_{\min}, x_{\max}]$. Let define the exploration sphere $\mathcal{C}_E$ of center $A = (0, l_0)$ and radius $R = l_1 + l_2$ corresponding of the distance the ROV can theoretically move due to the limitation of its umbilical length (*i.e.* outside of area F).

In general case, a configuration where $l_0 = y_{\text{floor}}$ and a ratio $\frac{F_{b2}}{F_{b1}} = \frac{l_1}{l_2}$ is recommended. Specifics configurations are proposed below.

Case 1: sea exploration at great depth

Suppose here the ROV explore the sea and is deep enough such the surface is inaccessible, *i.e.* the ROV can not reach the surface and areas B and C don't exist. For a chosen $x_{\max}$ and $[y_{\min}, y_{\max}]$, takes $l_1 = \frac{1}{2}\sqrt{x_{\max}^2 + (y_{\max}-y_{\min})^2}$, $l_2 = l_1$, $F_{b1} = F_{b2}$ and

- if the seafloor is accessible and $y_{\max} = y_{\text{floor}}$, takes $l_0 = y_{\text{floor}}$,
- if the seafloor is inaccessible or $y_{\max} \neq y_{\text{floor}}$, takes $l_0 = \frac{y_{\max}+y_{\min}}{2}$.

Note if the seafloor is inaccessible, it is recommend to choose an other umbilical management strategy, for example one of the strategies described in [21].

Case 2: exploration at shallow depth

Suppose now the surface is accessible and so can be a constraint for the ROV displacement. In case where $x_{\max} > y_{\max} - y_{\min}$, a compromise must be made. Since the boat can move on the surface, $(y_{\min}, y_{\max})$ are favored over $x_{\max}$to guarantee the umbilical stays stretched. To guarantee

$(y_{\min}, y_{\max})$ for the largest x possible, takes $l_0 = y_{\max}$, $l_2 = (y_{\max} + y_{\min}) - l_1$ with

$$l_1 = \frac{1}{\left(\frac{F_{b1}}{F_{b2}} + 1\right)} (y_{\max} + y_{\min}) \tag{62}$$

where $F_{b1} \geq F_{b2}$ if we desire to explore the sea, $F_{b1} < F_{b2}$ if we desire to explore the seafloor, following the idea which will be exposed in cases 3 and 4. Proof of (62) is provided in Appendix L2.

Case 3: seafloor exploration

Suppose here the ROV needs to explore the seafloor and this one is few uneven with small obstacles. Suppose also the surface is inaccessible. The main objective here is to explore a large area of radius $x_{\max}$ at $y = y_{\max} = y_{\text{floor}}$ or close: $x_{\max}$ is here favored over $y_{\min}$. For a small $y_{\min}$, one takes $l_0 = y_{\text{floor}}$, $l_2 = y_{\text{floor}} - y_{\min}$, $l_1 = \sqrt{l_2^2 + x_{\max}^2}$ and $F_{b2} > F_{b1}$ such F_{b2} is taken big compare to F_{b1} (example: $F_{b2} = 5F_{b1}$). An example is provided in Figure 5 a.

Note in case where the surface is accessible, remind $l_1 \leq l_0$, and for a given l_2, the minimum depth $y_{\min} = l_2 - 2(l_0 - l_1)$ must be respected.

Case 4: seafloor exploration with presence of large obstacles

Suppose here the ROV needs to explore an uneven seafloor with large/high obstacles. To avoid the umbilical comes in contact with an obstacle, parameters are proposed to keep the cable l_2 close to the vertical. Suppose again the surface is inaccessible.

For the area $[x_{\min}, x_{\max}] \times [y_{\min}, y_{\text{floor}}]$ where the ROV must explore, takes $l_0 = y_{\min} - h_A$ where h_A is the anchor A: the anchor is not inside the exploration area and so cannot come into contact with an obstacle.

Let define $\beta_{\max}$ a chosen parameters such we desire that $\forall x \in [x_{\min}, x_{\max}]$, $\beta \leq \beta_{\max}$, *i.e.* $\beta_{\max}$characterizes the verticality of l_2. To keep both buoys $B1$ and $B2$ outside the exploration area, for a couple (F_{b1}, F_{b2}) such $F_{b2} > F_{b1}$, takes

$$l_2 = \frac{y_{\text{floor}} - l_0}{\cos(\beta_{\max})} \tag{63}$$

$$l_1 = (x_{\max} - l_2 \sin(\beta_{\max})) \sqrt{1 + \left(\frac{1}{\tan(\beta_{\max})} \Lambda_{A2}\right)^2}. \tag{64}$$

The proof of (64) is provided in Appendix L1. An example illustrates theses parameters in Figure 5 b for $F_{b2} = 5F_{b1}$ and $\beta_{\max} = 10°$.

In case where the surface is accessible, remind $l_1 \leq l_0$ and $y_{\min} = l_2 - 2(l_0 - l_1)$ must be respected.

IV. Practical case

A. 3-Dimensionnal case and presence of horizontal current

In absence of horizontal current, the three dimensions case can be simply solved using the two dimensions case. Let define the 3D referential $\mathcal{R}_{3D} = (x, y, z)$ of origin $O = (0, 0, 0)$, where y is the vertical axis oriented to the ground. $(x, 0, z)$ is the horizontal plan at the sea level. $(x, y, 0)$ is the vertical plan such $\vec{OR}.\vec{z} = 0$, where $\vec{OR}$ is the vector between the boat and the ROV. One observes the umbilical is always at the equilibrium inside $(x, y, 0)$, so the solution of the 3D case without current is the solution of the 2D-case performed inside $(x, y, 0)$.

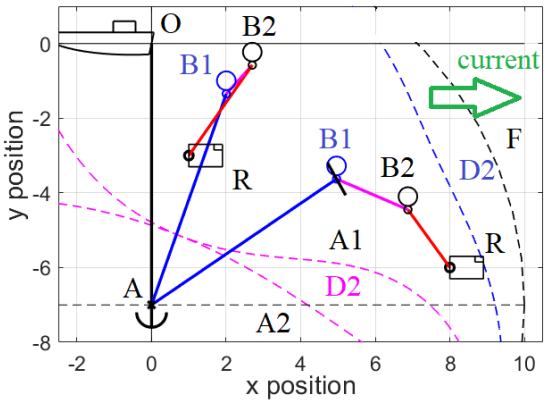

Fig. 6: Two examples of the method with horizontal current. Risk of entanglement on the left tether.

The presence of a horizontal current makes the system asymmetrical and changes the position of the buoys, as well as the shape of the areas presented in Section III-A. In the 2D-case, it can lead to entanglement if the ROV is closed to the cable l_0, see example Figure 6. In the 3D-case, the risk of entanglement decreases when the cable is oriented perpendicularly to the current, because buoys are pushed in a direction perpendicular to their functional displacement. In this case, the umbilical model is much more complex to define and describe. An example has been studied in [21] for a fixed ballast and a sliding buoy, but the problem is here more complex due to the two sliding elements. It will be the object of future works. However, note that if the forces of the buoys are much stronger than the horizontal currents, their effects can be neglected.

The vertical currents have already been treated in Assumption A5.

B. Quasi-static equilibrium: ROV control

The systems presented in previous sections are studied at the equilibrium. However, each time the ROV moves down, up or back, a part of the umbilical becomes temporary loosen. Since a loosen cable can lead to an entanglement and can be complex and/or heavy to compute, an alternative approach is proposed here by controlling the ROV to shorten the transitory phases and to decrease the discrepancy between the models studied and the reality. Thus, the ROV is controlled to move slower than the rise of the buoy. As long as their behaviors are faster than the ROV's velocity, the umbilical stays globally taut.

Details of this approach is described in [21].

C. Umbilical in presence of waves

In presence of waves, the position O of the boat becomes sinusoidal, impacting the position of the anchor A, and then

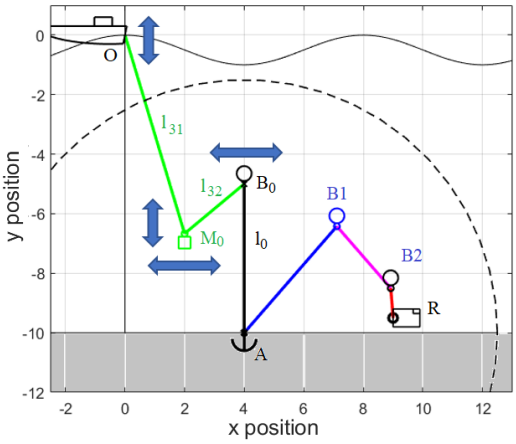

Fig. 7: System to counter-balance wave effect on the umbilical and the ROV. Green: additional cable l_3, fixed buoy $B0$ and sliding ballast $M0$. The system in green allows to prevent waves' effects in the umbilical between A and R and avoid cable breakage.

buoys' positions and forces inside the umbilical. When the anchor does not touch the seafloor, this one can keep the umbilical stretched during the descent phase if its weight allowing it to accelerate and fall faster than the wave, as more described in the Section 9 in [21]. However, in case where the anchor touches the seafloor (permanently by choice or temporally due to the waves' oscillations), the umbilical cannot be kept taut continuously, which can be dangerous for the material and lead to a cable breakage.

To avoid this problem, this section proposes a strategy to counter the wave's effect on the umbilical between the anchor and the ROV while avoiding an umbilical breakage, illustrated in Figure 7. Here, the umbilical between the boat O and the anchor A is divides in two parts. The first part l_3 between the boat and a fixed buoy $B0$, the second l_0 between the buoy $B0$ and the anchor A. A sliding ballast $M0$ can move freely on the cable l_3 between O and A. The force of the ballast is chosen such it can accelerate and fall faster than the wave but stay smaller than the buoy's strength. Moreover, the anchor's weight is much stronger than the force of buoy $B0$. The anchor A is put on the seafloor at y_{floor}. Since the influence of waves is maximum at the surface and decreases with depth, to become negligible, the length l_0 is chosen such direct waves influence on the buoys $B0$, $B1$ and $B2$ is negligible, $i.e.$ one has at least $l_0 < y_{\text{floor}} - 2h_w$ where h_w the wave's height. Finally, the length l_3 is chosen such the ballast can never touch the seafloor and cannot come in contact with the buoy $B0$, $i.e.$ $l_3 < y_{\text{floor}} - (h_w + h_B)$ and $y_{\text{floor}} + h_w < l_3 + l_0$ where h_B the ballast height.

Using the system previously described, when boat moves due to the action of the wave, the sliding ballast falls or works in opposition to keep the cable l_3 stretched in all situations, while the buoy $B0$ oscillates to absorb the waves' effect, and the anchor stays immobile on the seafloor. Since the anchor stays immobile, no action from the waves affects the part of the umbilical between A and R.

Finally, the launching of the system is not more complicated than for the system described in Section III because the buoy $B0$ is carried away by the anchor since this one hasn't touched the seafloor and the ballast $M0$ sinks to stay in contact with the buoy $B0$ during the launching: the umbilical stays perfectly stretched between the anchor and the boat. When the anchor reaches the seafloor, the ballast naturally slides along the cable l_3 since this one is completely unrolled. Sames steps work during the winding.

V. Experimental tests

This section discusses the validity of the assumptions made in the paper, exposes some problems in practical case and provides some experimental results to illustrate the validity of the study.

A. Validity of assumptions taken and choice of ballast and buoy

Consider first the assumptions made in this study. The Assumptions A1, A4, A5 and A6 can easily be respected by the choice of the buoy volume. Assumption A7 can be respected easily if the anchor is on the seafloor or in absence of horizontal current, but presence of strong horizontal current or waves can make it invalid and will be subject of futures studies. Presence of horizontal current on all the system, more complex, will be the subject of future studies too.

However, the Assumptions A2 and A3 can be satisfied for l_1 and l_2 only when the umbilical is relatively short (50m or less between the points). Moreover, to respect A2 for the cable l_0 and avoid too strong constrain on it due to its length and anchor in practice, the umbilical can be attached to a chain such the chain supports the anchor and the deformation while the extremity of the umbilical l_1 starts at the anchor.

Assumption A6 considers the friction between the umbilical and the sliding ballast/buoy is quite negligible to allow the ballast/buoy to reach its theoretical equilibrium position. A pulley has been used in practice to let the buoy slide with few friction, as illustrated in Figure 8. Tests show Assumption A6 can be respected mostly, but cannot be taken lightly, see next section. Note the radium of the pulley R_p must be taken larger than the radius made by cable rigidity, involving to take $R_{curve} = R_p$. The buoy is linked to the pulley by a mechanical ball joint to avoid twist force on the umbilical by the buoy.

The choice of the buoys can be more complex, because they must be taken such the umbilical weight/buoyancy is negligent compare to it, and can be deformed by them. Theoretically, any couple of two buoys respecting ratio $\frac{F_{b1}}{F_{b2}}$ works, however the biggest the buoys are, the fastest the dynamic of the system is but the strongest the force applied on the ROV by the umbilical is too. Moreover, the buoys must be taken such the umbilical respects A1 and A2: choice of the ballast and buoy is a trade-off between perturbation on the ROV, its maximum velocity and cable parameters.

B. Materials and experimentation

As illustrated in Figure 9, the configuration has been tested in pool of size $3m \times 4m$ with a depth of $3m$, in absence of

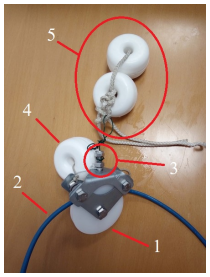

Fig. 8: Pulley to obtain a sliding buoy. 1: pulley. 2: umbilical. 3: ball joint to reduce twist effort between the buoy and the pulley. 4: additional buoy and ballast to give a neutral buoyancy to the pulley assembly (without considering the buoys in 5). 5: buoy for the self-management strategy.

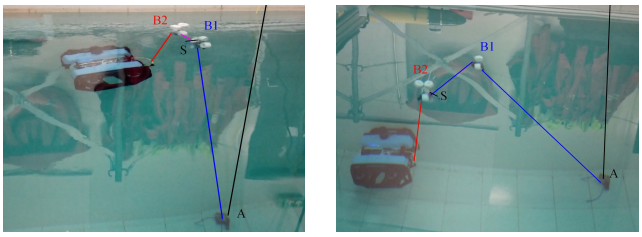

(a) ROV in area A1 (b) ROV in area A2

Fig. 9: Seafloor and diving exploration strategy, materials used for experimental tests in pool. Here, $F_{b1} = 135$g, $F_{b2} = 270$g, $l_0 = 3$m, $l_1 = 2$m and $l_2 = 1$m. Anchor: 1.5kg. One observes l_2 is close to the vertical when the ROV is close to the seafloor, like in the theory.

current with a real ROV. To obtain a configuration immobile for the measurement presented in this section, the ROV has been replaced by an anchor immersed at a controlled distance and depth from the origin $(0, 0)$ (let however call it "ROV" in the text below), and the umbilical is replaced by a rope with the following characteristic: diameter 4mm, $R_{curve} = 18$mm, 1m weighs 60g. The pulley has an internal radius of $R_p = 20$mm. The measurement have been made with a measuring tape.

The force of a buoy is evaluated in gram, corresponding to the maximum mass it can lift. One takes the following parameters : $F_{b1} = 260$g , $F_{b2} = 520$g, $l_0 = 2.85$m, $l_1 = 2.05$m, $l_2 = 2.05$m.

Let defined E_{B2} the discrepancy between the measured position $(x_{B2,m}, y_{B2,m})$ and its theoretical position $(x_{B2,th}, y_{B2,th})$ of the buoy $B2$ for a ROV position (x_{ROV}, y_{ROV}) such as

$$E_{B2}\left(x_{ROV}, y_{ROV}\right) = \sqrt{\left(x_{B2,th} - x_{B2,m}\right)^2 + \left(y_{B2,th} - y_{B2,m}\right)^2}. \tag{65}$$

Since the movement of the buoy $B2$ is larger than the movement of buoy $B1$, the accuracy of the method is studied using E_{B2}.

Figure 10a shows the difference between measured and theoretical areas B and C. One can observe that the experimental areas are close to the theoretical ones, the most important differences are mainly due to the measurement error: the boundary between areas B and C, $i.e.$ the beginning of the umbilical release, is not always simple to observe in practice. During the experiments, the boundary was measured when buoy $B1$ reached its rest position $(0, l_0 - l_1)$ or when the umbilical started to twist due to the lack of tension between the ballast and the buoy.

Figure 10b shows the discrepancy E_{B2} for several positions (x_{ROV}, y_{ROV}). The average value of E_{B2} is $E_{B2} = 0.128$m. Note that $E_{B2} = 0$ corresponds to the case when the cable is slack, $i.e.$ when the ROV is inside the area C and therefore cannot be compared to the proposed models. The values $E_{B2} = 0$ are not taken into account in the calculation of the average value.

These figures show that the discrepancy between the theoretical model and the experimental results is small when the ROV is close to the origin and becomes larger when it moves always. The first reason is the cable rigidity, which is not perfectly considered in the model, induces a small difference between the theoretical and measured angle. The second reason is that the tests show the frictions cannot be totally neglected, and thus the immobilization of the buoys $B1$ and $B2$ positions are not always identical depending on the starting point of the buoys and the movement performed by the ROV. The results shown in the Figure 10b are therefore the average of three measurements. One observes that the closer the cable is to the horizontal, the greater the friction problem: the friction is thus negligible when the ROV is close to the origin, which explain the results obtained. Note that since the friction slows the buoy when it approaches its equilibrium position, the measured error is likely independent of the length of the cable, making the relative error smaller for longer cable, although tests are needed to confirm this hypothesis. Note also that the rope used had a higher friction than a classic ROV's umbilical.

Despite the discrepancy between theory and practice, the umbilical remains perfectly taut during all tests since the ROV is outside the area C, even during the transition phases, and its shape is predictable with a margin error.

Two videos of the model in the pool and its reversed version at sea are available at https://youtu.be/BfcRRaSGlJA and https://youtu.be/XKg3x7TRrpU.

VI. Conclusion

This work proposes a passive self-management strategy of the umbilical for a ROV using sliding buoys and stop to tend the umbilical without motorization.

The strategy allows an exploration of the sea and seafloor exploration in presence of high obstacle. Compared to methods studied in previous works, this strategy has smallest restriction areas thank to the exclusive use of sliding element and stop, allowing to combine several fixed elements configurations in one. Two-dimensional model of the umbilical shape has been provided, considering absence of horizontal currents. Cables are assimilated to straight lines with minimum angle between them to consider umbilical rigidity. Several areas have been defined where the umbilical behavior are different, guarantying with a limitation of the ROV's velocity a safe exploration

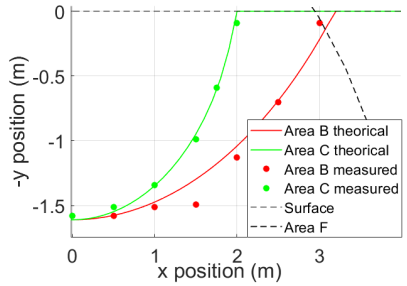

(a) Areas B and C. Plain lines: theoretical areas. Dots: experimental measurement.

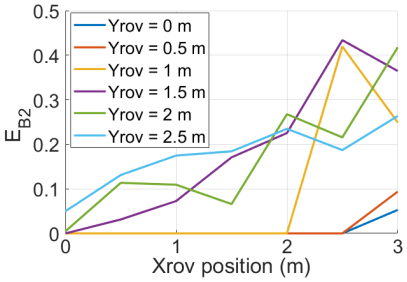

(b) Error E_{B2}. Average value of E_{B2}: $E_{B2} = 0.128$m.

Fig. 10: Experimental measurements. Each point is the average of three measurements for the same position (x_{ROV}, y_{ROV}).

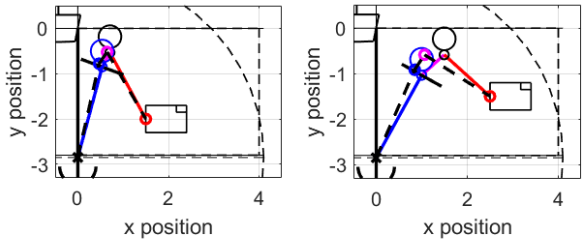

(a) Left: $E_{B2} = 0.098$m. Right: $E_{B2} = 0.434$m

Fig. 11: Comparison between theoretical umbilical (colored plain lines) and measured umbilical (large dash black lines) for diving exploration strategy. Small black dash lines: poolside. The left configuration is an example of small discrepancy and the right is the largest discrepancy of the experimentation.

without risk of entanglement on the umbilical itself. The forces applied on the umbilical and the ROV have been evaluated, and methods to choice umbilical parameters have been proposed. Finally, experimentation show the effectiveness and limits of the models due to the presence of friction. A strategy to counter-balance the effect of waves is also proposed. The ROV's velocity is limited to keep the quasi-static equilibrium valid in all configurations.

Future works will study these configuration in presence of horizontal current, presence of waves and uncertainty on parameters. More experimentation with measurements in sea during will be performed.

Acknowledgment

We acknowledge support from the Centre National de la Recherche Scientifique (CNRS) and Laboratoire des sciences et techniques de l'information, de la communication et de la connaissance (Lab-STICC). The author declares that there is no conflict of interest.

References

[1] BA Abel. Underwater vehicle tether management systems. In *Proceedings of OCEANS'94*, volume 2, pages II–495, 1994.

[2] O. Blintsov. Development of the mathematical modeling method for dynamics of the flexible tether as an element of the underwater complex. *Eastern-European Journal of Enterprise Technologies*, 1 (7):4–14, 2017.

[3] L. Brignone, E. Raugel, J. Opderbecke, V. Rigaud, R. Piasco, and S. Ragot. First sea trials of hrov the new hybrid vehicle developed by ifremer. In *Oceans 2015-genova*, pages 1–7, 2015.

[4] B. Buckham and M. Nahon. Dynamics simulation of low tension tethers. In *IEEE Conference Proceedings Oceans*, volume 2, pages 757–766, 1999.

[5] R. D. Christ and R. L. Wernli Sr. *The ROV manual: a user guide for observation class remotely operated vehicles*. Elsevier, 2011.

[6] T. Crandle, G. Cook, and E. Celkis. Tradeoffs between umbilical and battery power in rov performance. In *IEEE OCEANS 2017-Anchorage*, pages 1–6, 2017.

[7] R. G. Duncan, Mark E. Froggatt, S. .T Kreger, R. J. Seeley, D. K. Gifford, A. K. Sang, and M. S. Wolfe. High-accuracy fiber-optic shape sensing. In *Sensor Systems and Networks*, volume 6530, page 65301S, 2007.

[8] O. A. Eidsvik and I. Schjølberg. Time domain modeling of rov umbilical using beam equations. *IFAC*, 49(23):452–457, 2016.

[9] O. A. N. Eidsvik and I. Schjølberg. Finite element cable-model for remotely operated vehicles (rovs) by application of beam theory. *Ocean Engineering*, 163:322–336, 2018.

[10] J. E. Frank, R. Geiger, D. R. Kraige, and A. Murali. Smart tether system for underwater navigation and cable shape measurement, 2013. US Patent 8,437,979, URL https://patents.google.com/patent/US8437979B2/en.

[11] O. Ganoni, R. Mukundan, and R. Green. Visually realistic graphical simulation of underwater cable. 2018.

[12] F. González, A. de la Prada, A. Luaces, and M. González. Real-time simulation of cable pay-out and reel-in with towed fishing gears. *Ocean Engineering*, 131:295–307, 2017.

[13] Sung Min Hong, Kyoung Nam Ha, and Joon-Young Kim. Dynamics modeling and motion simulation of usv/uuv with linked underwater cable. *Journal of Marine Science and Engineering*, 8(5):318, 2020.

[14] M. Laranjeira, C. Dune, and V. Hugel. Catenary-based visual servoing for tethered robots. In *IEEE International Conference on Robotics and Automation*, pages 732–738, 2017.

[15] M. Laranjeira, C. Dune, and V. Hugel. Embedded visual detection and shape identification of underwater umbilical for vehicle positioning. In *OCEANS 2019-Marseille*, pages 1–9, 2019.

[16] M. Laranjeira, C. Dune, and V. Hugel. Catenary-based visual servoing for tether shape control between underwater vehicles. *Ocean Engineering*, 200:107018, 2020.

[17] A. Lasbouygues, S. Louis, B. Ropars, L. Rossi, H. Jourde, H. Délas, P. Balordi, R. Bouchard, M. Dighouth, M. Dugrenot, et al. Robotic mapping of a karst aquifer. In *IFAC: International Federation of Automatic Control*, 2017.

[18] H. Stuart, S. Wang, O. Khatib, and M. R. Cutkosky. The ocean one hands: An adaptive design for robust marine manipulation. *The International Journal of Robotics Research*, 36(2):150–166, 2017.

[19] M. Such, J. R. Jimenez-Octavio, A. Carnicero, and O. Lopez-Garcia. An approach based on the catenary equation to deal with static analysis of three dimensional cable structures. *Engineering structures*, 31(9):2162–2170, 2009.

[20] O. Tortorici, C. Anthierens, V. Hugel, and H. Barthelemy. Towards active self-management of umbilical linking rov and usv for safer submarine missions. *IFAC-PapersOnLine*, 52(21):265–270, 2019.

[21] C. Viel. Self-management of the umbilical of a rov for underwater exploration. *Ocean Engineering*, 248:110695, 2022.

APPENDIX

A. Proof of Theorem 1

Let's study the system

$$\begin{cases} x = l_a \sin(\theta_a) + l_b \sin(\theta_b) \\ \tan(\theta_b) = \Lambda_{ab} \tan(\theta_a). \end{cases}$$

For a given θ, one has $\sin(\text{atan}(\theta)) = \frac{\theta}{\sqrt{1+\theta^2}}$, so

$$\begin{aligned} \sin(\theta_b) &= \sin(\text{atan}(\Lambda_{ab} \tan(\theta_a))) \\ &= \frac{\Lambda_{ab} \tan(\theta_a)}{\sqrt{1 + (\Lambda_{ab} \tan(\theta_a))^2}}. \end{aligned} \tag{66}$$

Put $X = \sin(\theta_a)$. Thus, one has

$$\tan(\theta_a) = \frac{X}{\sqrt{1 - X^2}} \tag{67}$$

and so (66) becomes

$$\begin{aligned} \sin(\theta_b) &= \frac{\frac{\Lambda_{ab} X}{\sqrt{1-X^2}}}{\sqrt{1 + \left(\frac{\Lambda_{ab} X}{\sqrt{1-X^2}}\right)^2}} \\ &= \frac{\Lambda_{ab} X}{\sqrt{1 + (\Lambda_{ab}^2 - 1) X^2}}. \end{aligned} \tag{68}$$

By introducing (18) and (17) inside (14), one gets

$$x = l_a \sin(\theta_a) + l_b \sin(\theta_b). \tag{69}$$

Let's introduce X and (68) inside (69):

$$x = l_a X + \frac{l_b \Lambda_{ab} X}{\sqrt{1 + (\Lambda_{ab}^2 - 1) X^2}}$$

$$(x - l_a X) \sqrt{1 + (\Lambda_{ab}^2 - 1) X^2} = l_b \Lambda_{ab} X$$

$$(x - l_a X)^2 \left(1 + (\Lambda_{ab}^2 - 1) X^2\right) = (l_b \Lambda_{ab} X)^2$$

$$\left(x^2 - 2x l_a X + l_a^2 X^2\right) \left(1 + (\Lambda_{ab}^2 - 1) X^2\right) = l_b^2 \Lambda_{ab}^2 X^2$$

$$\begin{aligned} x^2 + x^2 (\Lambda_{ab}^2 - 1) X^2 - 2x l_a X - 2x l_a (\Lambda_{ab}^2 - 1) X^3 \\ + l_a^2 X^2 + l_a^2 (\Lambda_{ab}^2 - 1) X^4 - l_b^2 \Lambda_{ab}^2 X^2 = 0 \end{aligned} \tag{70}$$

which can be reorganised such

$$a X^4 + b X^3 + c X^2 + d X + E = 0 \tag{71}$$

with

$$a = l_a^2 (\Lambda_{ab}^2 - 1) \tag{72}$$

$$b = -2 x l_a (\Lambda_{ab}^2 - 1) \tag{73}$$

$$c = x^2 (\Lambda_{ab}^2 - 1) - l_b^2 \Lambda_{ab}^2 + l_a^2 \tag{74}$$

$$d = -2 x l_a \tag{75}$$

$$e = x^2. \tag{76}$$

(71) is a quartic function which can be solved using Ludovico Ferrari, described for our parameters in Section B.

Remark if $\Lambda_{ab}^2 = 1$, one has $a = 0$ and $b = 0$. (71) becomes a second order polynomial whom the solution which interest us is

$$\sin(\gamma) = \frac{-d - \sqrt{d^2 - 4ce}}{2c} \tag{77}$$

which is equal to

$$\begin{aligned} \sin(\gamma) &= \frac{x (l_a - l_b)}{l_a^2 - l_b^2}. \\ &= \frac{x (l_a - l_b)}{(l_a - l_b)(l_a + l_b)} \\ &= \frac{x}{(l_a + l_b)}. \end{aligned} \tag{78}$$

B. Solve quartic function

Considering our application, only one solution of the quartic function corresponds to our configuration. This section summarized the Ludovico Ferrari's method to solve quartic function and add the knowledge of ours parameters to exclude some cases and pick the appropriate solution.

Let solve the quartic function

$$a X^4 + b X^3 + c X^2 + d X + e = 0. \tag{79}$$

Suppose $a \neq 0$ and $b \neq 0$, so $\Lambda_{ab} \neq 1$, else the solution of (71) is described in (77). Suppose also $x > 0$, else the only geometric solution is $X = 0$. Case $x < 0$ is treated in the Corollary 6.

Theorem 5. *Consider $x > 0$ and $\Lambda_{ab} \neq 1$. The solution of (79) considering the relation between the parameters l_a, l_b, x, Λ_{ab} is*

$$X = \min_{i \in [1,2,3,4]} (|X_i|) \, sgn(x) \tag{80}$$

where

$$\begin{cases} X_1 = \frac{\sqrt{U - \frac{2}{3}A} - \sqrt{\Delta_{Y1}}}{2}, X_2 = \frac{\sqrt{U - \frac{2}{3}A} + \sqrt{\Delta_{Y1}}}{2}, \text{if } \Delta_{Y1} \geq 0 \\ X_1 = \infty, X_2 = \infty \quad \text{else,} \end{cases} \tag{81}$$

$$\begin{cases} X_3 = \frac{-\sqrt{U - \frac{2}{3}A} - \sqrt{\Delta_{Y2}}}{2}, X_4 = \frac{-\sqrt{U - \frac{2}{3}A} + \sqrt{\Delta_{Y2}}}{2}, \text{if } \Delta_{Y2} \geq 0 \\ X_3 = \infty, X_4 = \infty \quad \text{else,} \end{cases} \tag{82}$$

for $\Delta_{Y1} = -\left(U + \frac{4}{3}A + \frac{2B}{\sqrt{U - \frac{2}{3}A}}\right)$ *and* $\Delta_{Y2} = -\left(U + \frac{4}{3}A - \frac{2B}{\sqrt{U - \frac{2}{3}A}}\right)$ *with*

$$A = -\frac{x^2}{2l_a^2} - \frac{\left(l_b^2 \Lambda_{ab}^2 - l_a^2\right)}{l_a^2 (\Lambda_{ab}^2 - 1)} \tag{83}$$

$$B = -\frac{l_a^2 + l_b^2 \Lambda_{ab}^2}{l_a^3 (\Lambda_{ab}^2 - 1)} x \tag{84}$$

$$C = \frac{x^4}{16 l_a^4} + \frac{x^2 \left(l_a^2 - l_b^2 \Lambda_{ab}^2\right)}{4 l_a^4 (\Lambda_{ab}^2 - 1)} \tag{85}$$

$$U = \begin{cases} \left(-\frac{q}{2} + \sqrt{\frac{q^2}{4} + \frac{p^3}{27}}\right)^{\frac{1}{3}} + \left(-\frac{q}{2} - \sqrt{\frac{q^2}{4} + \frac{p^3}{27}}\right)^{\frac{1}{3}} & \text{if } \Delta_U > 0, \\ 2 \cos\left(\frac{1}{3} acos\left(-\frac{q}{2\sqrt{-\frac{p^3}{27}}}\right)\right) \sqrt{-\frac{p}{3}} & \text{if } \Delta_U < 0, \\ -\sqrt{-\frac{p}{3}} & \text{if } \Delta_U = 0 \end{cases} \tag{86}$$

with $\Delta_U = \frac{q^2}{4} + \frac{p^3}{27}$, $p = -4C - \frac{A^2}{3}$ *and* $q = \frac{2A^3}{27} + \left(4AC - B^2\right) + \frac{-4CA}{3}$.

Corollary 6. *The Theorem 5 can be extended to the case* $x < 0$ *by taking* $|x|$ *instead of* x *inside the Theorem 5 and take the solution* $\sin(\gamma_A) = \min_{i\in[1,2,3,4]}(|X_i|)\, sgn(x)$.

1) Proof of Theorem 5

: Suppose here $x > 0$, $\Lambda_{ab} \neq 1$, $a \neq 0$ and $b \neq 0$. By putting $X = Y - \frac{b}{4a}$, (79) becomes

$$Y^4 + AY^2 + BY + C = 0 \tag{87}$$

with

$$A = \frac{-3b^2}{8a^2} + \frac{c}{a} \tag{88}$$

$$B = \frac{\left(\frac{b}{2}\right)^3}{a^3} - \frac{1}{2}\frac{bc}{a^2} + \frac{d}{a} \tag{89}$$

$$C = -3\left(\frac{b}{4a}\right)^4 + c\frac{\left(\frac{b}{4}\right)^2}{a^3} - \frac{1}{4}\frac{bd}{a^2} + \frac{e}{a}. \tag{90}$$

Let show that in our case, $B \neq 0$. We introduce the value of (72)-(76) inside B:

$$\begin{aligned} B &= \frac{\left(\frac{b}{2}\right)^3}{a^3} - \frac{1}{2}\frac{bc}{a^2} + \frac{d}{a} \\ &= \frac{\left(-xl_a\left(\Lambda_{ab}^2 - 1\right)\right)^3}{\left(l_a^2\left(\Lambda_{ab}^2 - 1\right)\right)^3} + \frac{-2xl_a}{l_a^2\left(\Lambda_{ab}^2 - 1\right)} \\ &\quad - \frac{1}{2}\frac{\left(-2xl_a\left(\Lambda_{ab}^2 - 1\right)\right)\left(x^2\left(\Lambda_{ab}^2 - 1\right) - l_b^2\Lambda_{ab}^2 + l_a^2\right)}{\left(l_a^2\left(\Lambda_{ab}^2 - 1\right)\right)^2} \\ &= -\left(\frac{x}{l_a}\right)^3 - \frac{2x}{l_a\left(\Lambda_{ab}^2 - 1\right)} + \frac{x\left(x^2\left(\Lambda_{ab}^2 - 1\right) - l_b^2\Lambda_{ab}^2 + l_a^2\right)}{l_a\left(\Lambda_{ab}^2 - 1\right)} \\ &= \frac{-x^2\left(\Lambda_{ab}^2 - 1\right) - 2l_a^2 + \left(x^2\left(\Lambda_{ab}^2 - 1\right) - l_b^2\Lambda_{ab}^2 + l_a^2\right)}{l_a\left(\Lambda_{ab}^2 - 1\right)}x \\ &= \frac{-l_a^2 - l_b^2\Lambda_{ab}^2}{l_a\left(\Lambda_{ab}^2 - 1\right)}x \end{aligned} \tag{91}$$

and since $x > 0$, $l_b > 0$, $l_a > 0$ and $\Lambda_{ab} \neq 1$, one has $B \neq 0$.

Since $B \neq 0$, (87) can be rewritten

$$\left(Y^2 + \frac{u}{2}\right)^2 = (u - A)(Y - Z)^2 \tag{92}$$

where $Z = \frac{B}{2(u-A)}$ and u is the solution of

$$\begin{aligned} u^3 - Au^2 - 4Cu + \left(4AC - B^2\right) &= 0 \\ \bar{a}u^3 + \bar{b}u^2 + \bar{c}u + \bar{d} &= 0 \end{aligned} \tag{93}$$

with

$$\bar{a} = 1 \tag{94}$$

$$\bar{b} = -A \tag{95}$$

$$\bar{c} = -4C \tag{96}$$

$$\bar{d} = 4AC - B^2. \tag{97}$$

and where (93) can be evaluated using **Cardan formula.**

a) Evaluation of u

: Using Cardan approach, (93) can be rewritten such that

$$U^3 + pU + q = 0 \tag{98}$$

where

$$u = \left(U - \frac{\bar{b}}{3\bar{a}}\right) = U + \frac{A}{3} \tag{99}$$

$$p = \left(\frac{\bar{c}}{\bar{a}} - \frac{\bar{b}^2}{3\bar{a}^2}\right) = -4C - \frac{A^2}{3} \tag{100}$$

$$q = \left(\frac{2\bar{b}^3}{27\bar{a}^3} + \frac{\bar{d}}{\bar{a}} - \frac{\bar{b}\bar{c}}{3\bar{a}^2}\right) = \frac{2A^3}{27} + \left(4AC - B^2\right) + \frac{-4CA}{3} \tag{101}$$

Still following the Cardan approach, let define the determinant $\Delta_U = \frac{q^2}{4} + \frac{p^3}{27}$ and consider cases $\Delta_U > 0$, $\Delta_U < 0$ and $\Delta_U = 0$:

- If $\Delta_U > 0$, p and q are necessarily negative (property of Cardan formula) and the solution of (98) is

$$U = \left(-\frac{q}{2} + \sqrt{\frac{q^2}{4} + \frac{p^3}{27}}\right)^{\frac{1}{3}} + \left(-\frac{q}{2} - \sqrt{\frac{q^2}{4} + \frac{p^3}{27}}\right)^{\frac{1}{3}} \tag{102}$$

  and so $U > 0$.
- If $\Delta_U < 0$, one has necessarily $p < 0$ (property of Cardan formula) and the solution of (98) is

$$U = 2\cos\left(\frac{t}{3}\right)\sqrt{-\frac{p}{3}} \tag{103}$$

  with

$$t = \operatorname{acos}\left(-\frac{q}{2r}\right) \tag{104}$$

$$r = \sqrt{-\frac{p^3}{27}} \tag{105}$$

  and so $U > 0$.
- If $\Delta_U = 0$, one has necessarily $p < 0$ (property of Cardan formula) and the solution of (98) is

$$U = \sqrt{-\frac{p}{3}}. \tag{106}$$

  and $U \geq 0$.

b) Evaluation of Y

: Let's go back to (92):

$$\left(Y^2 + \frac{u}{2}\right)^2 = (u - A)(Y - Z)^2 \tag{107}$$

with

$$\begin{aligned} Z &= \frac{B}{2(u - A)} \\ &= \frac{B}{2\left(U - \frac{2A}{3}\right)}. \end{aligned} \tag{108}$$

Y of (107) is the solution of one of the two equations

$$\begin{cases} Y^2 + \frac{u}{2} = T(Y - Z) \\ Y^2 + \frac{u}{2} = -T(Y - Z) \end{cases} \tag{109}$$

with $T=\sqrt{u-A}$ and $Z=\frac{B}{2(u-A)}$

$$\begin{cases} Y^2-YT+\left(ZT+\frac{u}{2}\right)=0 \\ Y^2+YT+\left(-ZT+\frac{u}{2}\right)=0. \end{cases} \tag{110}$$

For (110), we can define two discriminates Δ_{Y1} and Δ_{Y2}. Consider first Δ_{Y1}

$$\begin{aligned}\Delta_{Y1} &= T^2-4\left(ZT+\frac{u}{2}\right) \\ &= (u-A)-4\left(\frac{B\sqrt{u-A}}{2\left(U-\frac{2A}{3}\right)}+\frac{u}{2}\right).\end{aligned} \tag{111}$$

Since $u=U+\frac{A}{3}$, one gets

$$\begin{aligned}\Delta_{Y1} &= \left(U-\frac{2}{3}A\right)-4\left(\frac{B\sqrt{U-\frac{2}{3}A}}{2\left(U-\frac{2A}{3}\right)}+\frac{U}{2}+\frac{1}{6}A\right) \\ &= \left(U-\frac{2}{3}A\right)-\left(\frac{2B}{\sqrt{U-\frac{2}{3}A}}+2U+\frac{2}{3}A\right) \\ &= -\left(U+\frac{4}{3}A+\frac{2B}{\sqrt{U-\frac{2}{3}A}}\right).\end{aligned} \tag{112}$$

In the same way, one can get

$$\Delta_{Y2}=-\left(U+\frac{4}{3}A-\frac{2B}{\sqrt{U-\frac{2}{3}A}}\right). \tag{113}$$

and obtain the four solution of (110):

$$Y_1=\frac{\sqrt{U-\frac{2}{3}A}-\sqrt{\Delta_{Y1}}}{2} \tag{114}$$

$$Y_2=\frac{\sqrt{U-\frac{2}{3}A}+\sqrt{\Delta_{Y1}}}{2} \tag{115}$$

$$Y_3=\frac{-\sqrt{U-\frac{2}{3}A}-\sqrt{\Delta_{Y2}}}{2} \tag{116}$$

$$Y_4=\frac{-\sqrt{U-\frac{2}{3}A}+\sqrt{\Delta_{Y2}}}{2}. \tag{117}$$

Remind $X=Y-\frac{b}{4a}$, so $X=Y+\frac{x}{2l_a}$. Then from (114)-(117), one gets the four solution X_k for $k\in[1,\ldots,4]$:

$$X_1=\frac{\sqrt{U-\frac{2}{3}A}-\sqrt{\Delta_{Y1}}}{2} \tag{118}$$

$$X_2=\frac{\sqrt{U-\frac{2}{3}A}+\sqrt{\Delta_{Y1}}}{2} \tag{119}$$

$$X_3=\frac{-\sqrt{U-\frac{2}{3}A}-\sqrt{\Delta_{Y2}}}{2} \tag{120}$$

$$X_4=\frac{-\sqrt{U-\frac{2}{3}A}+\sqrt{\Delta_{Y2}}}{2}. \tag{121}$$

For our case, the solution is the smallest real absolute value of the X_k solution, so

$$X=\min_{i\in[1,2,3,4]}\left(|X_i|\right). \tag{122}$$

c) Simplification of C :

$$\begin{aligned}C &= -3\left(\frac{b}{4a}\right)^4+c\frac{\left(\frac{b}{4}\right)^2}{a^3}-\frac{1}{4}\frac{bd}{a^2}+\frac{e}{a}. \\ &= -3\left(\frac{-2xl_a\left(\Lambda_{ab}^2-1\right)}{4l_a^2\left(\Lambda_{ab}^2-1\right)}\right)^4 \\ &+\frac{\left(x^2\left(\Lambda_{ab}^2-1\right)-l_b^2\Lambda_{ab}^2+l_a^2\right)}{\left(l_a^2\left(\Lambda_{ab}^2-1\right)\right)^3}\left(\frac{-2xl_a\left(\Lambda_{ab}^2-1\right)}{4}\right)^2 \\ &-\frac{1}{4}\frac{\left(-2xl_a\left(\Lambda_{ab}^2-1\right)\right)\left(-2xl_a\right)}{\left(l_a^2\left(\Lambda_{ab}^2-1\right)\right)^2}+\frac{x^2}{l_a^2\left(\Lambda_{ab}^2-1\right)} \\ &= -3\frac{x^4}{16l_a}+\frac{\left(x^2\left(\Lambda_{ab}^2-1\right)-l_b^2\Lambda_{ab}^2+l_a^2\right)}{l_a\left(\Lambda_{ab}^2-1\right)^3} \\ &\times\left(\frac{x^2l_a^2\left(\Lambda_{ab}^2-1\right)^2}{4}\right)-\frac{\left(xl_a\right)^2\left(\Lambda_{ab}^2-1\right)}{l_a\left(\Lambda_{ab}^2-1\right)^2}+\frac{x^2}{l_a^2\left(\Lambda_{ab}^2-1\right)} \\ &= -\frac{3}{16}\frac{x^4}{l_a}+\frac{\left(x^2\left(\Lambda_{ab}^2-1\right)-l_b^2\Lambda_{ab}^2+l_a^2\right)}{l_a\left(\Lambda_{ab}^2-1\right)}\left(\frac{x^2}{4}\right) \\ &-\frac{x^2}{l_a^2\left(\Lambda_{ab}^2-1\right)}+\frac{x^2}{l_a^2\left(\Lambda_{ab}^2-1\right)} \\ &= -\frac{3}{16}\frac{x^4}{l_a}+\frac{x^4\left(\Lambda_{ab}^2-1\right)-x^2l_b^2\Lambda_{ab}^2+x^2l_a^2}{4l_a\left(\Lambda_{ab}^2-1\right)} \\ &= -\frac{3x^4\left(\Lambda_{ab}^2-1\right)}{16l_a}+\frac{4x^4\left(\Lambda_{ab}^2-1\right)-4x^2l_b^2\Lambda_{ab}^2+4x^2l_a^2}{16l_a\left(\Lambda_{ab}^2-1\right)} \\ &= \frac{x^4\left(\Lambda_{ab}^2-1\right)-4x^2l_b^2\Lambda_{ab}^2+4x^2l_a^2}{16l_a\left(\Lambda_{ab}^2-1\right)} \\ &= \frac{x^4}{16l_a}+\frac{x^2\left(l_a^2-l_b^2\Lambda_{ab}^2\right)}{4l_a\left(\Lambda_{ab}^2-1\right)}\end{aligned} \tag{123}$$

C. Proof of (22)

Suppose the system is in a configuration where the buoys are not in contact, the buoy $B1$ is in contact with the stop S and the buoy $B2$ is not in contact with the ROV or the surface, so $\gamma\in\left[0,\frac{\pi}{2}\right[$. Note these conditions are satisfied in area A1.

From (20), one gets

$$\Sigma_{B1}\vec{F}.\vec{x}=-T_1\sin(\gamma)+T_2\sin(-\alpha) \tag{124}$$

$$\Sigma_{B1}\vec{F}.\vec{y}=-F_{b1}+T_1\cos(\gamma)-T_2\cos(-\alpha). \tag{125}$$

Consider first $\gamma\neq 0$ and remark from (124) that $\alpha\neq 0$ if $\gamma\neq 0$ since $T_1\neq 0$ and $T_2\neq 0$, and so $\beta\neq 0$ from (18). Since $\Sigma_{B1}\vec{F}.\vec{x}=0$ and $\Sigma_{B1}\vec{F}.\vec{y}=0$, one gets from (124)-(125)

$$T_1=T_2\frac{\sin(-\alpha)}{\sin(\gamma)} \tag{126}$$

$$T_1\cos(\gamma)=F_{b1}+T_2\cos(-\alpha) \tag{127}$$

and since $\gamma\in\left]0,\frac{\pi}{2}\right[$ here, one has by combining (126) and (127):

$$\begin{aligned}T_2\frac{\sin(-\alpha)}{\tan(\gamma)} &= F_{b1}+T_2\cos(-\alpha) \\ F_{b1} &= T_2\left[-\cos(-\alpha)+\frac{\sin(-\alpha)}{\tan(\gamma)}\right].\end{aligned} \tag{128}$$

Similarly, one gets from (21)

$$\Sigma_{B2}\vec{F}.\vec{x} = -T_3\sin(\beta) + T_2\sin(-\alpha) \tag{129}$$

$$\Sigma_{B2}\vec{F}.\vec{y} = -F_{b2} + T_3\cos(\beta) + T_2\cos(-\alpha) \tag{130}$$

In area A1, one has (18) so $\alpha = -\beta$. Thus, since $\Sigma_{B2}\vec{F}.\vec{x} = 0$ and $\Sigma_{B2}\vec{F}.\vec{y} = 0$, one gets

$$T_3 = T_2 \tag{131}$$

$$F_{b2} = 2\cos(\beta)\,T_2 \tag{132}$$

From (128) and (132), one gets

$$\begin{aligned}\frac{F_{b2}}{2\cos(\beta)} &= \frac{F_{b1}}{\left[-\cos(-\alpha) + \frac{\sin(-\alpha)}{\tan(\gamma)}\right]}\\ \frac{2F_{b1}}{F_{b2}} &= \frac{1}{\cos(\beta)}\left[-\cos(\beta) + \frac{\sin(\beta)}{\tan(\gamma)}\right]\\ \frac{2F_{b1}}{F_{b2}} + 1 &= \frac{\tan(\beta)}{\tan(\gamma)}\\ \tan(\beta) &= \left(\frac{2F_{b1}}{F_{b2}} + 1\right)\tan(\gamma).\end{aligned} \tag{133}$$

Consider now $\gamma = 0$. Since $\Sigma_{B1}\vec{F}.\vec{x} = 0$ and $\Sigma_{B1}\vec{F}.\vec{y} = 0$, one gets from (124) that $T_2\sin(-\alpha) = 0$, inducing $\alpha = 0$ or $\alpha = \pi$. In area A1, one has (18) so $\alpha = -\beta$, thus $\beta = 0$ or $\beta = \pi$. In both case, one has $\tan(\beta) = \tan(\gamma) = 0$, so (133) is still true.

D. Proof of (23)

Suppose the system is in a configuration where the buoys are not in contact, the buoy $B1$ is not in contact with the stop S or the surface and the buoy $B2$ is in contact with the stop, so $\gamma \in \left[0, \frac{\pi}{2}\right[$. Note these conditions are satisfied in area A2. From (20), one gets

$$\Sigma_{B2}\vec{F}.\vec{x} = -T_3\sin(\beta) + T_2\sin(-\alpha) \tag{134}$$

$$\Sigma_{B2}\vec{F}.\vec{y} = -F_{b2} + T_3\cos(\beta) - T_2\cos(-\alpha). \tag{135}$$

Consider first $\beta \neq 0$ and remark from (134) that $\alpha \neq 0$ if $\beta \neq 0$ since $T_2 \neq 0$ and $T_3 \neq 0$, and so $\gamma \neq 0$ from (19). Since $\Sigma_{B2}\vec{F}.\vec{x} = 0$ and $\Sigma_{B2}\vec{F}.\vec{y} = 0$, one gets from (134)-(135)

$$T_3 = T_2\frac{\sin(-\alpha)}{\sin(\beta)} \tag{136}$$

$$T_3\cos(\beta) = F_{b2} + T_2\cos(-\alpha) \tag{137}$$

and since $\beta \in \left]0, \frac{\pi}{2}\right[$ here, by combining (136) and (137), one gets

$$\begin{aligned}T_2\frac{\sin(-\alpha)}{\tan(\beta)} &= F_{b2} + T_2\cos(-\alpha)\\ F_{b2} &= T_2\left[-\cos(-\alpha) + \frac{\sin(-\alpha)}{\tan(\beta)}\right].\end{aligned} \tag{138}$$

Similarly, one gets from (21)

$$\Sigma_{B1}\vec{F}.\vec{x} = -T_1\sin(\gamma) + T_2\sin(-\alpha) \tag{139}$$

$$\Sigma_{B1}\vec{F}.\vec{y} = -F_{b1} + T_1\cos(\gamma) + T_2\cos(-\alpha). \tag{140}$$

In area A2, one has (19) so $\alpha = -\gamma$. Thus, since $\Sigma_{B1}\vec{F}.\vec{x} = 0$ and $\Sigma_{B1}\vec{F}.\vec{y} = 0$, one gets

$$T_1 = T_2 \tag{141}$$

$$F_{b1} = 2\cos(\gamma)\,T_2 \tag{142}$$

From (138) and (142), one gets

$$\begin{aligned}\frac{F_{b1}}{2\cos(\gamma)} &= \frac{F_{b2}}{\left[-\cos(-\alpha) + \frac{\sin(-\alpha)}{\tan(\beta)}\right]}\\ \frac{2F_{b2}}{F_{b1}} &= \frac{1}{\cos(\gamma)}\left[-\cos(\gamma) + \frac{\sin(\gamma)}{\tan(\beta)}\right]\\ \frac{2F_{b2}}{F_{b1}} + 1 &= \frac{\tan(\gamma)}{\tan(\beta)}\\ \tan(\gamma) &= \left(\frac{2F_{b2}}{F_{b1}} + 1\right)\tan(\beta)\end{aligned} \tag{143}$$

or

$$\tan(\beta) = \frac{1}{\left(\frac{2F_{b2}}{F_{b1}} + 1\right)}\tan(\gamma) \tag{144}$$

Consider now $\beta = 0$. Since $\Sigma_{B2}\vec{F}.\vec{x} = 0$ and $\Sigma_{B2}\vec{F}.\vec{y} = 0$, one gets from (134) that $T_2\sin(-\alpha) = 0$, inducing $\alpha = 0$ or $\alpha = \pi$. In area A2, one has (19) so $\alpha = -\gamma$, thus $\gamma = 0$ or $\gamma = \pi$. In both case, one has $\tan(\beta) = \tan(\gamma) = 0$, so (144) is still true.

E. Calculation of γ in area A1

Since $F_{b1} > 0$ and $F_{b2} > 0$, one has $\Lambda_{A1} = 2\frac{F_{b1}}{F_{b2}} + 1 > 1$. Moreover, by introducing (18) and (17) inside (14), one gets

$$x = l_1\sin(\gamma) + l_2\sin(\beta). \tag{145}$$

Considering the parameters $l_a = l_1$, $l_b = L$, $\Lambda_{ab} = \Lambda_{A1}$, $\theta_a = \gamma$ and $\theta_b = \beta$, one has $l_a > 0$, $l_b > 0$, $\Lambda_{ab} > 0$. Thus the solution of (145) is $\sin(\gamma) = F(x, l_1, l_2, \Lambda_{A1}) = F(x, l_a, l_b, \Lambda_{ab})$, where $F(x, l_a, l_b, \Lambda_{ab})$ is solution exposed in Theorem 1.

F. Calculation of l_{21} and l_{22} in area A1

Suppose β and γ have been previously evaluated using (18) and results of Appendix E. Since $l_{11} = l_1$, $l_{12} = 0$ in area A1, (15) can be rewritten such

$$\begin{aligned}y &= l_0 - l_1\cos(\gamma) + l_{21}\cos(\beta) + (l_2 - l_{21})\cos(\beta)\\ y &= l_0 - l_1\cos(\gamma) + (l_2 - 2l_{21})\cos(\beta)\\ -2l_{21} &= -l_2 + \frac{y - l_0 + l_1\cos(\gamma)}{\cos(\beta)}\\ l_{21} &= \frac{l_2}{2} - \frac{y - l_0 + l_1\cos(\gamma)}{2\cos(\beta)}\end{aligned} \tag{146}$$

and so $l_{22} = l_2 - l_{21}$.

G. Calculation of γ in area A2

Since $F_{b1} > 0$ and $F_{b2} > 0$, one has $\Lambda_{A2} = \frac{1}{2\frac{F_{b2}}{F_{b1}}+1} > 0$. Moreover, by introducing (16) and (19) inside (14), one gets

$$x = l_1 \sin(\gamma) + l_2 \sin(\beta). \tag{147}$$

Considering the parameters $l_a = l_1$, $l_b = l_2$, $\Lambda_{ab} = \Lambda_{A2}$, $\theta_a = \gamma$ and $\theta_b = \beta$, one has $l_a > 0$, $l_b > 0$, $\Lambda_{ab} > 0$. Thus the solution of (147) is $\sin(\gamma) = F(x, l_1, l_2, \Lambda_{A2}) = F(x, l_a, l_b, \Lambda_{ab})$, where $F(x, l_a, l_b, \Lambda_{ab})$ is solution exposed in Theorem 1.

H. Calculation of l_{11} and l_{12} in area A2

Suppose β and γ have been previously evaluated using (18) and results of Appendix G. Since $l_{21} = 0$, $l_{22} = l_2$ in area A2, (15) can be rewritten such

$$\begin{aligned} y &= l_0 - l_{11}\cos(\gamma) + (l_1 - l_{11})\cos(\gamma) + l_2\cos(\beta) \\ y &= l_0 - 2l_{11}\cos(\gamma) + l_1\cos(\gamma) + l_2\cos(\beta) \\ 2l_{11}\cos(\gamma) &= l_1\cos(\gamma) + l_0 - y + l_2\cos(\beta) \\ l_{11} &= \frac{l_1}{2} + \frac{l_0 - y + l_2\cos(\beta)}{2\cos(\gamma)} \end{aligned} \tag{148}$$

and so $l_{12} = l_1 - l_{11}$.

I. Calculation of the boundary between areas

1) Boundary areas A1-B: $y = l_{22}\cos(\beta) + h_{b2}$: The boundary between the areas A1 and B corresponds to the depth $y = l_{22}\cos(\beta) + h_{b2}$ with $l_{22} \geq 0$ because the buoy $B2$ is on the surface without being in contact with the ROV. One still has $l_{11} = l_1$ and $l_{12} = 0$ at the boundary. Since $\beta = -\alpha$ in area A1 and B, (15) becomes

$$\begin{aligned} l_{22}\cos(\beta) + h_{b2} &= l_0 - l_1\cos(\gamma) - l_{21}\cos(\alpha) + l_{22}\cos(\beta) \\ h_{b2} &= l_0 - l_1\cos(\gamma) - l_{21}\cos(\beta) \\ l_{21} &= \frac{l_0 - h_{b2} - l_1\cos(\gamma)}{\cos(\beta)} \end{aligned} \tag{149}$$

and since $l_2 = l_{21} + l_{22}$, one gets

$$l_{22} = l_2 - \frac{l_0 - h_{b2} - l_1\cos(\gamma)}{\cos(\beta)}. \tag{150}$$

At the boundary of areas A1 and B, β can still be evaluated using (18) and γ_{A1} can be evaluated using Theorem 2. Let $\gamma_{A1}(x)$ be the value of γ inside the area A1 for a position x. Thus, one has

$$\begin{aligned} \cos(\beta) &= \cos\left(\operatorname{atan}\left(\Lambda_{A1}\tan(\gamma_{A1}(x))\right)\right) \\ &= \frac{1}{\sqrt{1 + \Lambda_{A1}^2\tan(\gamma_{A1}(x))^2}}. \end{aligned} \tag{151}$$

Using (150) and (151), for a given x, the associate depth y_{areaB} can be expressed as

$$\begin{aligned} &y_{area\,B}(x) \\ &= \max\left([l_{22}\cos(\beta), 0]\right) + h_{b2} \\ &= \max\left([l_2\cos(\beta) + l_1\cos(\gamma_{A1}(x)) - l_0 + 2h_{b2}, h_{b2}]\right) \\ &= \max\left(\left[\frac{l_2}{\sqrt{1 + \Lambda_{A1}^2\tan(\gamma_{A1}(x))^2}}\right.\right. \\ &\left.\left. + l_1\cos(\gamma_{A1}(x)) - l_0 + 2h_{b2}, h_{b2}\right]\right). \end{aligned} \tag{152}$$

Remark $y_{area\,B}$ can be rewritten such

$$\begin{aligned} &y_{area\,B}(x) = \\ &\max\left(\left[\frac{l_2 + l_1\sqrt{1 + (\Lambda_{A1}^2 - 1)\sin(\gamma_{A1}(x))^2}}{\sqrt{1 + \Lambda_{A1}^2\tan(\gamma_{A1}(x))^2}}\right.\right. \\ &\left.\left. - l_0 + 2h_{b2}, h_{b2}\right]\right) \end{aligned} \tag{153}$$

with $\Lambda_{A1} > 1$.

Let's now study (153) and find a condition where $y_{area\,B}(x)$ is always lower to h_{b2}:

$$\frac{l_2 + l_1\sqrt{1 + (\Lambda_{A1}^2 - 1)\sin(\gamma_A(x))^2}}{\sqrt{1 + \Lambda_{A1}^2\tan(\gamma_{A1}(x))^2}} - l_0 + 2h_{b2} \leq h_{b2}$$

$$\begin{aligned} &l_2 + l_1\sqrt{1 + (\Lambda_{A1}^2 - 1)\sin(\gamma_{A1}(x))^2} \\ &\leq (l_0 - h_{b2})\sqrt{1 + \Lambda_{A1}^2\tan(\gamma_{A1}(x))^2} \end{aligned}$$

$$\begin{aligned} l_2 \leq &\sqrt{1 + \Lambda_{A1}^2\tan(\gamma_{A1}(x))^2}(l_0 - h_{b2}) \\ &- l_1\sqrt{1 + (\Lambda_{A1}^2 - 1)\sin(\gamma_{A1}(x))^2}. \end{aligned} \tag{154}$$

and (154) is always respected if

$$l_2 \leq (l_0 - h_{b2}) - l_1. \tag{155}$$

Thus, (155) shows the area B exists only if $l_2 > l_0 - (l_1 + h_{b2})$. Else, one can take $y_{area\,B}(x) = 0$ because the area does not exist, *i.e.* the buoy can not reach the surface.

One can so write

$$\begin{aligned} &y_{area\,B}(x) = \\ &\begin{cases} \max\left(\left[\frac{l_2 + l_1\sqrt{1 + \left(\Lambda_{A1}^2 - 1\right)\sin(\gamma_{A1}(x))^2}}{\sqrt{1 + \Lambda_{A1}^2\tan(\gamma_{A1}(x))^2}}\right.\right. \\ \left.\left. - l_0 + 2h_{b2}, h_{b2}\right]\right) & \text{if } l_2 > l_0 - (h_{b2} + l_1) \\ 0 & \text{else.} \end{cases} \end{aligned} \tag{156}$$

and the ROV is inside the area B if $y < y_{area\,B}(x)$.

2) Boundary areas B-C

: The area C can correspond to the cases where the buoy $B2$ is on the surface but the cable l_1 is vertical ($\gamma = 0$), so the buoy $B1$ can not taut the cable l_2. In this configuration, area B exists and we search the boundary between the areas B and C. At the boundary of the two areas, the buoy $B2$ is on the surface and the buoy $B1$ can still taut the cable l_2. In absence of current, the buoy $B1$ can apply a tension simultaneously on the cable l_{11} and $l_{12} + l_2$ only for angles γ such $\gamma \in \left[0, \frac{\pi}{2}s\right]$, where $s = \text{sgn}(x)$. The boundary between the two areas correspond so to the instant when $\gamma = 0$, the last position before the buoy $B1$ cannot stretch the cable. Let's studied the system for $\gamma = 0$.

When $\gamma = 0$, the buoy $B1$ is in contact with the stop, so $l_{11} = l_1$ and $l_{12} = 0$. Since (18) is still valid at the boundary between areas B and C, one can deduce from (14) that

$$x = l_1 \sin(\gamma) + l_2 \sin(\beta) \tag{157}$$

and for $\gamma = 0$, one gets

$$\sin(\beta) = \frac{x}{l_2}, \tag{158}$$

which is possible only if $x \leq l_2$.

Put the condition $x \leq l_2$. Since the buoy $B1$ is on the surface, one has $y = l_{22}\cos(\beta) + h_{b2}$. From (15) and since (18) and $\gamma = 0$, one gets

$$\begin{aligned} y &= l_0 - l_1\cos(\gamma) - l_{21}\cos(\beta) + l_{22}\cos(\beta) \\ h_{b2} &= l_0 - l_1 - l_{21}\cos\left(\text{asin}\left(\frac{x}{l_2}\right)\right) \\ l_{21} &= \frac{l_0 - h_{b2} - l_1}{\sqrt{1 - \frac{x^2}{l_2^2}}}. \end{aligned} \tag{159}$$

and $l_{22} = l_2 - l_{21}$.

Introducing (159) into $y = l_{22}\cos(\beta) + h_{b2}$, one gets if $x \leq l_2$

$$\begin{aligned} &y_{area\,C}(x) \\ &= \max\left(\left[\left(l_2 - \frac{l_0 - h_{b2} - l_1}{\sqrt{1 - \frac{x^2}{l_2^2}}}\right)\sqrt{1 - \frac{x^2}{l_2^2}}, 0\right]\right) + h_{b2} \\ &= \max\left(\left[\sqrt{l_2^2 - x^2} + l_1 - l_0 + 2h_{b2}, h_{b2}\right]\right) \end{aligned} \tag{160}$$

and $y_{area\,C}(x) = 0$ if $x > l_2$. Moreover, one can see from (160) that $y_{area\,C}(x) = h_{b2}$ for all x if $l_2 \leq l_0 - (l_1 + h_{b2})$, which confirm the existence of area B. Note one can take $y_{area\,C}(x) = 0$ if $l_2 \leq l_0 - (l_1 + h_{b2})$ because the buoy $B2$ cannot reach the surface so the area does not exist. Thus,

$$y_{area\,C}(x) = \begin{cases} \max\left(\left[\sqrt{l_2^2 - x^2} + l_1 \right.\right. \\ \left.\left. -l_0 + 2h_{b2}, h_{b2}\right]\right) & \text{if } (x \leq l_2)\,\&\,(l_2 > l_0 - l_1 + h_{b2}) \\ h_{b2} & \text{if } (x > l_2)\,\&\,(l_2 > l_0 - l_1 + h_{b2}) \\ 0 & \text{else.} \end{cases} \tag{161}$$

3) Boundary areas A1-D1

: In the area D1, the buoy $B2$ is in contact with the ROV, so $l_{22} = 0$ and $l_{21} = l_2$, and the buoy $B1$ with the stop, thus $l_{11} = l_1$ and $l_{12} = 0$. The system (14)-(15) becomes

$$x = l_1 \sin(\gamma) - l_2 \sin(\alpha) \tag{162}$$

$$y = l_0 - l_1\cos(\gamma) - l_2\cos(\alpha). \tag{163}$$

At the boundary of areas A1 and D1, one still have (18), *i.e.* $\beta = -\alpha$, and β can still be evaluated using (22) and γ_{A1} can be evaluated using Theorem 2. Let $\gamma_{A1}(x)$ be the value of γ inside the area A1 for a position x. Thus, one has

$$\begin{aligned} \cos(\beta) &= \cos\left(\text{atan}\left(\Lambda_{A1}\tan\left(\gamma_{A1}(x)\right)\right)\right) \\ &= \frac{1}{\sqrt{1 + \Lambda_{A1}^2\tan\left(\gamma_{A1}(x)\right)^2}}. \end{aligned} \tag{164}$$

Using (164) and (163), the depth $y_{area\,D1}$ can be expressed for a given x as

$$\begin{aligned} &y_{area\,D1}(x) \\ &= \max\left(\left[l_0 - l_1\cos\left(\gamma_{A1}(x)\right) - l_2\cos(\beta), 0\right]\right) \\ &= \max\left(\left[l_0 - l_1\cos\left(\gamma_{A1}(x)\right)\right.\right. \\ &\quad \left.\left. - \frac{l_2}{\sqrt{1 + \Lambda_{A1}^2\tan\left(\gamma_{A1}(x)\right)^2}}, 0\right]\right). \end{aligned} \tag{165}$$

The ROV is inside the area $D1$ if $y < y_{area\,D1}(x)$. Remark (165) can be rewritten such

$$\begin{aligned} &y_{area\,D1}(x) = \\ &\max\left(\left[l_0 - \frac{l_1\sqrt{1 + (\Lambda_{A1}^2 - 1)\sin\left(\gamma_{A1}(x)\right)^2} + l_2}{\sqrt{1 + \Lambda_{A1}^2\tan\left(\gamma_{A1}(x)\right)^2}}, 0\right]\right). \end{aligned} \tag{166}$$

4) Boundary areas A1-D2

: In the area D2, the buoys $B1$ and $B2$ are in contact with the stop, so $l_{11} = l_1$, $l_{12} = 0$ $l_{22} = l_2$ and $l_{21} = 0$. Thus (14)-(15) becomes

$$x = l_1 \sin(\gamma) + l_2 \sin(\beta) \tag{167}$$

$$y = l_0 - l_1\cos(\gamma) + l_2\cos(\beta). \tag{168}$$

At the boundary of areas A1 and D2, β can still be evaluated using (22) and γ can be evaluated using Theorem 2 such $\gamma = \gamma_{A1}$, where $\gamma_{A1}(x)$ is the value of γ inside the area A1 for a position x. From (22), one gets

$$\begin{aligned} \cos(\beta) &= \cos\left(\text{atan}\left(\Lambda_{A1}\tan\left(\gamma_{A1}(x)\right)\right)\right) \\ &= \frac{1}{\sqrt{1 + \Lambda_{A1}^2\tan\left(\gamma_{A1}(x)\right)^2}}. \end{aligned} \tag{169}$$

Thus, using (169) and (168), for a given x, the depth

$y_{area\ A1-D2}$ can be expressed as

$$\begin{aligned} & y_{area\ A1-D2}(x) \\ & = \max\left(\left[l_0 - l_1\cos\left(\gamma_{A1}(x)\right) + l_2\cos\left(\beta\right), 0\right]\right) \\ & = \max\left(\left[l_0 - l_1\cos\left(\gamma_{A1}(x)\right)\right.\right. \\ & \left.\left. + \frac{l_2}{\sqrt{1+\Lambda_{A1}^2\tan\left(\gamma_{A1}(x)\right)^2}}, 0\right]\right). \end{aligned} \tag{170}$$

The ROV enters inside the area D2 from area A1 when y becomes lower than $y_{area\ A1-D2}(x)$. Remark (170) can be rewritten such

$$y_{area\ A1-D2}(x) = \max\left(\left[l_0 + \frac{-l_1\sqrt{1+\left(\Lambda_{A1}^2-1\right)\sin\left(\gamma_{A1}(x)\right)^2}+l_2}{\sqrt{1+\Lambda_{A1}^2\tan\left(\gamma_{A1}(x)\right)^2}}, 0\right]\right). \tag{171}$$

5) Boundary areas A2-D2

: In the area D2, the buoys $B1$ and $B2$ are in contact with the stop, so $l_{11} = l_1$, $l_{12} = 0$ $l_{22} = l_2$ and $l_{21} = 0$. Thus (14)-(15) becomes

$$x = l_1\sin\left(\gamma\right) + l_2\sin\left(\beta\right) \tag{172}$$

$$y = l_0 - l_1\cos\left(\gamma\right) + l_2\cos\left(\beta\right). \tag{173}$$

At the boundary of areas A2 and D2, β can still be evaluated using (23) and γ can be evaluated using Theorem 3 such $\gamma = \gamma_{A2}$, where $\gamma_{A2}(x)$ is the value of γ inside the area A2 for a position x. From (23), one gets

$$\begin{aligned} \cos\left(\beta\right) &= \cos\left(\text{atan}\left(\Lambda_{A2}\tan\left(\gamma_{A2}(x)\right)\right)\right) \\ &= \frac{1}{\sqrt{1+\Lambda_{A2}^2\tan\left(\gamma_{A2}(x)\right)^2}}. \end{aligned} \tag{174}$$

Thus, using (174) and (173), for a given x, the depth $y_{area\ A2-D2}$ can be expressed as

$$\begin{aligned} & y_{area\ A2-D2}(x) \\ & = \max\left(\left[l_0 - l_1\cos\left(\gamma_{A2}(x)\right) + l_2\cos\left(\beta\right), 0\right]\right) \\ & = \max\left(\left[l_0 - l_1\cos\left(\gamma_{A2}(x)\right)\right.\right. \\ & \left.\left. + \frac{l_2}{\sqrt{1+\Lambda_{A2}^2\tan\left(\gamma_{A2}(x)\right)^2}}, 0\right]\right). \end{aligned} \tag{175}$$

The ROV enters inside the area D2 from area A2 when y becomes higher than $y_{area\ A2-D2}(x)$. Remark (175) can be rewritten such

$$y_{area\ A2-D2}(x) = \max\left(\left[l_0 + \frac{-l_1\sqrt{1+\left(\Lambda_{A2}^2-1\right)\sin\left(\gamma_{A2}(x)\right)^2}+l_2}{\sqrt{1+\Lambda_{A2}^2\tan\left(\gamma_{A2}(x)\right)^2}}, 0\right]\right). \tag{176}$$

6) Boundary areas A2-D3

: In area D3, the buoy $B1$ is in contact with the anchor and the buoy $B2$ with the stop, so $l_{11} = 0$, $l_{12} = l_1$, $l_{22} = l_2$ and $l_{21} = 0$. Thus (14)-(15) becomes

$$x = -l_1\sin\left(\alpha\right) + l_2\sin\left(\beta\right) \tag{177}$$

$$y = l_0 + l_1\cos\left(\alpha\right) + l_2\cos\left(\beta\right). \tag{178}$$

At the boundary of areas A2 and D3, β can still be evaluated using (23), (19) induces $\alpha = -\gamma$ and γ can be evaluate using Theorem 3 such $\gamma = \gamma_{A2}$, where $\gamma_{A2}(x)$ is the value of γ inside the area A2 for a position x. From (23), one gets

$$\begin{aligned} \cos\left(\beta\right) &= \cos\left(\text{atan}\left(\Lambda_{A2}\tan\left(\gamma_{A2}(x)\right)\right)\right) \\ &= \frac{1}{\sqrt{1+\Lambda_{A2}^2\tan\left(\gamma_{A2}(x)\right)^2}}. \end{aligned} \tag{179}$$

Thus, using (23), (179) and (178), for a given x, the depth $y_{area\ D3}$ can be expressed as

$$\begin{aligned} & y_{area\ D3}(x) \\ & = \max\left(\left[l_0 + l_1\cos\left(\gamma_{A2}(x)\right) + l_2\cos\left(\beta\right), 0\right]\right) \\ & = \max\left(\left[l_0 + l_1\cos\left(\gamma_{A2}(x)\right) + \right.\right. \\ & \left.\left. + \frac{l_2}{\sqrt{1+\Lambda_{A2}^2\tan\left(\gamma_{A2}(x)\right)^2}}, 0\right]\right). \end{aligned} \tag{180}$$

The ROV is inside the area D3 if $y > y_{area\ D3}(x)$. Remark (180) can be rewritten such

$$y_{area\ D3}(x) = \max\left(\left[l_0 + \frac{l_1\sqrt{1+\left(\Lambda_{A2}^2-1\right)\sin\left(\gamma_{A2}(x)\right)^2}+l_2}{\sqrt{1+\Lambda_{A2}^2\tan\left(\gamma_{A2}(x)\right)^2}}, 0\right]\right). \tag{181}$$

7) Boundary areas F

: The limit for the area F is simple because it corresponds to the maximum length of umbilical. The ROV is always outside the area F in practice because it can not physically go inside. The ROV is not inside the area F if $y_{area\ F1}(x) \leq y \leq y_{area\ F2}(x)$ where

$$y_{area\ F1}(x) = \max\left(l_0 - \sqrt{\left(l_1+L\right)^2 - x^2},\, 0\right). \tag{182}$$

$$y_{area\ F2}(x) = l_0 + \sqrt{\left(l_1+L\right)^2 - x^2}. \tag{183}$$

J. Calculation of γ, α and β

1) Calculation of γ, α and β in area D1

: Inside the area D1, the buoy $B1$ is in contact with the stop and the buoy $B2$ is in contact with the ROV, so $l_{11} = l_1$, $l_{12} = 0$, $l_{21} = l_2$ and $l_{22} = 0$. Moreover, one has $|\gamma| \in \left[0, \frac{\pi}{2}\right]$ and $\beta = 0$.

Consider first here $y - l_0 \neq 0$. Thus (14)-(15) becomes

$$x = l_1\sin\left(\gamma\right) - l_2\sin\left(\alpha\right) \tag{184}$$

$$y = l_0 - l_1\cos\left(\gamma\right) - l_2\cos\left(\alpha\right). \tag{185}$$

From (185), one gets

$$\cos\left(\alpha\right) = \frac{-y + l_0 - l_1\cos\left(\gamma\right)}{l_2} \tag{186}$$

and so by the oriented angle convention

$$\alpha = -\text{sgn}\,(x)\,\text{acos}\left(\frac{-y+l_0-l_1\cos(\gamma)}{l_2}\right). \quad (187)$$

Let find now γ. From (186) and (187), one has

$$\sin(\alpha) = -\sqrt{1-\left(\frac{-y+l_0-l_1\cos(\gamma)}{l_2}\right)^2} \quad (188)$$

By putting $X = \sin(\gamma)$, (188) becomes

$$\sin(\alpha) = -\frac{1}{l_2}\sqrt{l_2^2-\left(-y+l_0-l_1\sqrt{1-X^2}\right)^2}. \quad (189)$$

Introducing (189) inside (184), one gets

$$x = l_1X + l_2\left(\frac{1}{l_2}\sqrt{l_2^2-\left(-y+l_0-l_1\sqrt{1-X^2}\right)^2}\right) \quad (190)$$

which can be rewritten such

$$\begin{aligned}(x-l_1X)^2 &= l_2^2-\left(-(y-l_0)-l_1\sqrt{1-X^2}\right)^2\\ x^2-2l_1xX+l_1^2X^2 &= l_2^2-\Big((l_0-y)^2+2(y-l_0)l_1\sqrt{1-X^2}\\ &\quad +l_1^2-l_1^2X^2\Big)\\ x^2+(l_0-y)^2+l_1^2-l_2^2-2l_1xX &= -2(y-l_0)l_1\sqrt{1-X^2}\end{aligned}$$

$$\frac{x^2+(l_0-y)^2+l_1^2-l_2^2}{2(y-l_0)l_1}-\frac{x}{(y-l_0)}X = -\sqrt{1-X^2}$$

$$a_D - b_DX = -\sqrt{1-X^2} \quad (191)$$

where $a_D = \frac{x^2+(l_0-y)^2+l_1^2-l_2^2}{2(y-l_0)l_1}$ and $b_D = \frac{x}{(y-l_0)}$. (191) can be solved by studying

$$\begin{aligned}(a_D-b_DX)^2 &= 1-X^2\\ a_D^2-2a_Db_DX+b_D^2X^2 &= 1-X^2\\ a_D^2-1-2a_Db_DX+\left(1+b_D^2\right)X^2 &= 0\\ C_D-B_DX+A_DX^2 &= 0\end{aligned} \quad (192)$$

with $C_D = a_D^2-1$, $B_D = 2a_Db_D$ and $A_D = 1+b_D^2$. The two solutions of (192) are

$$\begin{aligned}X_{1D} &= \frac{B_D-\sqrt{B_D^2-4A_DC_D}}{2A_D}\\ &= \frac{a_Db_D-\sqrt{a_D^2b_D^2-(1+b_D^2)(a_D^2-1)}}{(1+b_D^2)}\end{aligned} \quad (193)$$

and

$$X_{2D} = \frac{a_Db_D+\sqrt{a_D^2b_D^2-(1+b_D^2)(a_D^2-1)}}{(1+b_D^2)} \quad (194)$$

and from (191), one can deduce the solution $X = \sin(\gamma)$ correspond to $X = X_i$ for $i \in \{1,2\}$ such $a_D - b_DX_i = -\sqrt{1-X_i^2}$. Thus,

$$\sin(\gamma) = \begin{cases} X_{1D} & \text{if } (T_{1D}==True)\,\&\,(T_{2D}==False)\\ X_{2D} & \text{if } (T_{1D}==False)\,\&\,(T_{2D}==True)\\ \min([X_{1D},\,X_{1D}]) & \text{if } (T_{1D}==True)\,\&\,(T_{2D}==True)\end{cases} \quad (195)$$

where $T_{1D} = \left(a_D - b_DX_{1D} == -\sqrt{1-X_{1D}^2}\right)$ and $T_{2D} = \left(a_D - b_DX_{2D} == -\sqrt{1-X_{2D}^2}\right)$.

Consider now the case $y - l_0 = 0$, and $x \neq 0$. Following the same steps, one gets

$$\cos(\alpha) = \frac{-l_1\cos(\gamma)}{l_2} \quad (196)$$

$$\sin(\gamma) = \frac{x^2+l_1^2-l_2^2}{2l_1x}. \quad (197)$$

2) Calculation of γ, α and β in area D2 : Inside the area D2, the buoys $B1$ and $B2$ are in contact with the stop, so $l_{11} = l_1$, $l_{12} = 0$, $l_{21} = 0$ and $l_{22} = l_2$. Moreover, one has $|\gamma| \in \left[0, \frac{\pi}{2}\right]$ and $\alpha = 0$.

Consider first here $y - l_0 \neq 0$. Thus (14)-(15) becomes

$$x = l_1\sin(\gamma) + l_2\sin(\beta) \quad (198)$$

$$y = l_0 - l_1\cos(\gamma) + l_2\cos(\beta). \quad (199)$$

From (199), one gets

$$\cos(\beta) = \frac{y-l_0+l_1\cos(\gamma)}{l_2} \quad (200)$$

and so by the oriented angle convention

$$\beta = \text{sgn}\,(x)\,\text{acos}\left(\frac{y-l_0+l_1\cos(\gamma)}{l_2}\right). \quad (201)$$

Let find now γ. From (200) and (201), one has

$$\sin(\beta) = \sqrt{1-\left(\frac{y-l_0+l_1\cos(\gamma)}{l_2}\right)^2} \quad (202)$$

By putting $X = \sin(\gamma)$, (202) becomes

$$\sin(\beta) = \frac{1}{l_2}\sqrt{l_2^2-\left(y-l_0+l_1\sqrt{1-X^2}\right)^2}. \quad (203)$$

Introducing (203) inside (198), one gets

$$x = l_1X + l_2\left(\frac{1}{l_2}\sqrt{L^2-\left(y-l_0+l_1\sqrt{1-X^2}\right)^2}\right) \quad (204)$$

which can be rewritten such

$$\begin{aligned}(x-l_1X)^2 &= l_2^2-\left((y-l_0)+l_1\sqrt{1-X^2}\right)^2\\ x^2-2l_1xX+l_1^2X^2 &= l_2^2-\Big((l_0-y)^2+2(y-l_0)l_1\sqrt{1-X^2}\\ &\quad +l_1^2-l_1^2X^2\Big)\\ x^2+(l_0-y)^2+l_1^2-l_2^2-2l_1xX &= -2(y-l_0)l_1\sqrt{1-X^2}\end{aligned}$$

$$\frac{x^2+(l_0-y)^2+l_1^2-l_2^2}{2(y-l_0)l_1}-\frac{x}{(y-l_0)}X = -\sqrt{1-X^2}. \quad (205)$$

Putting $a_D = \frac{x^2+(l_0-y)^2+l_1^2-l_2^2}{2(y-l_0)l_1}$ and $b_D = \frac{x}{(y-l_0)}$, (205) can be solved by studying

$$\begin{aligned}(a_D-b_DX)^2 &= 1-X^2\\ a_D^2-2a_Db_DX+b_D^2X^2 &= 1-X^2\\ a_D^2-1-2a_Db_DX+\left(1+b_D^2\right)X^2 &= 0\\ C_D-B_DX+A_DX^2 &= 0\end{aligned} \quad (206)$$

with $C_D = a_D^2 - 1$, $B_D = 2a_D b_D$ and $A_D = 1 + b_D^2$. The two solutions of (206) are

$$X_{1D} = \frac{B_D - \sqrt{B_D^2 - 4A_D C_D}}{2A_D} = \frac{a_D b_D - \sqrt{a_D^2 b_D^2 - (1+b_D^2)(a_D^2-1)}}{(1+b_D^2)} \quad (207)$$

and

$$X_{2D} = \frac{a_D b_D + \sqrt{a_D^2 b_D^2 - (1+b_D^2)(a_D^2-1)}}{(1+b_D^2)} \quad (208)$$

and from (205), one can deduce the solution $X = \sin(\gamma)$ correspond to $X = X_i$ for $i \in \{1,2\}$ such $a_D - b_D X_i = -\sqrt{1-X_i^2}$. Thus,

$$\sin(\gamma) = \begin{cases} X_{1D} & \text{if } (T_{1D} == True)\,\&\,(T_{2D} == False) \\ X_{2D} & \text{if } (T_{1D} == False)\,\&\,(T_{2D} == True) \\ \min([X_{1D},\, X_{1D}]) & \text{if } (T_{1D} == True)\,\&\,(T_{2D} == True) \end{cases} \quad (209)$$

where $T_{1D} = \left(a_D - b_D X_{1D} == -\sqrt{1-X_{1D}^2}\right)$ and $T_{2D} = \left(a_D - b_D X_{2D} == -\sqrt{1-X_{2D}^2}\right)$.

Consider now the case $y - l_0 = 0$, and $x \neq 0$. Following the same steps, one gets

$$\cos(\beta) = \frac{l_1 \cos(\gamma)}{l_2} \quad (210)$$

$$\sin(\gamma) = \frac{x^2 + l_1^2 - l_2^2}{2 l_1 x}. \quad (211)$$

3) Calculation of γ, α and β in area D3 : Inside the area D3, the buoy $B1$ is in contact with the anchor and the buoy $B2$ with the stop, so $l_{11} = 0$, $l_{12} = l_1$, $l_{21} = 0$, $l_{22} = l_2$ and $\gamma = 0$. Thus, (14)-(15) becomes

$$x = l_1 \sin(-\alpha) + l_2 \sin(\beta) \quad (212)$$

$$y = l_0 + l_1 \cos(\alpha) + l_2 \cos(\beta). \quad (213)$$

From (213), one gets

$$\cos(\beta) = \frac{y - l_0 - l_1 \cos(\alpha)}{l_2} \quad (214)$$

and so $\beta = \text{sgn}(x)\,\text{acos}\left(\frac{y-l_0-l_1\cos(\alpha)}{l_2}\right)$.

From (214), one has $\sin(\beta) = \sqrt{1 - \left(\frac{y-l_0-l_1\cos(\alpha)}{l_2}\right)^2}$. By putting $X = \sin(-\alpha)$, one gets

$$\sin(\beta) = \frac{1}{L}\sqrt{l_2^2 - \left(y - l_0 - l_1\sqrt{1-X^2}\right)^2}. \quad (215)$$

Introducing (203) inside (198), one gets

$$x = l_1 X + L\left(\frac{1}{L}\sqrt{l_2^2 - \left(y - l_0 - l_1\sqrt{1-X^2}\right)^2}\right) \quad (216)$$

which can be rewritten such

$$(x - l_1 X)^2 = l_2^2 - \left((y-l_0) - l_1\sqrt{1-X^2}\right)^2$$

$$x^2 - 2l_1 xX + l_1^2 X^2 = l_2^2 - \left((l_0-y)^2 - 2(y-l_0) l_1\sqrt{1-X^2} + l_1^2 - l_1^2 X^2\right)$$

$$x^2 + (l_0-y)^2 + l_1^2 - l_2^2 - 2l_1 xX = 2(y-l_0) l_1\sqrt{1-X^2}$$

$$\frac{x^2 + (l_0-y)^2 + l_1^2 - l_2^2}{2(y-l_0)l_1} - \frac{x}{(y-l_0)}X = \sqrt{1-X^2}$$

$$a_D - b_D X = \sqrt{1-X^2} \quad (217)$$

where $a_D = \frac{x^2+(l_0-y)^2+l_1^2-l_2^2}{2(y-l_0)l_1}$ and $b_D = \frac{x}{(y-l_0)}$. (191) can be solved by studying

$$(a_D - b_D X)^2 = 1 - X^2$$

$$a_D^2 - 2a_D b_D X + b_D^2 X^2 = 1 - X^2$$

$$a_D^2 - 1 - 2a_D b_D X + \left(1 + b_D^2\right) X^2 = 0$$

$$C_D - B_D X + A_D X^2 = 0 \quad (218)$$

with $C_D = a_D^2 - 1$, $B_D = 2a_D b_D$ and $A_D = 1 + b_D^2$. The two solutions of (218) are

$$X_{1D} = \frac{B_D - \sqrt{B_D^2 - 4A_D C_D}}{2A_D} = \frac{a_D b_D - \sqrt{a_D^2 b_D^2 - (1+b_D^2)(a_D^2-1)}}{(1+b_D^2)} \quad (219)$$

and

$$X_{2D} = \frac{a_D b_D + \sqrt{a_D^2 b_D^2 - (1+b_D^2)(a_D^2-1)}}{(1+b_D^2)} \quad (220)$$

and from (217), one can deduce the solution $X = \sin(\gamma)$ correspond to $X = X_i$ for $i \in \{1,2\}$ such $a_D - b_D X_i = \sqrt{1-X_i^2}$. Thus,

$$\sin(-\alpha) = \begin{cases} X_{1D} & \text{if } (T_3 == True)\,\&\,(T_4 == False) \\ X_{2D} & \text{if } (T_3 == False)\,\&\,(T_4 == True) \\ \min([X_{1D},\, X_{1D}]) & \text{if } (T_3 == True)\,\&\,(T_4 == True) \end{cases} \quad (221)$$

where $T_{3D} = \left(a_D - b_D X_{1D} == \sqrt{1-X_{1D}^2}\right)$ and $T_{4D} = \left(a_D - b_D X_{2D} == \sqrt{1-X_{2D}^2}\right)$.

4) Calculation of γ, α and β in area B : In area B, the buoy $B1$ is in contact with the stop and the buoy $B2$ is on the surface. $B1$ can still taut the cables l_1 and l_2, so $l_{11} = l_1$, $l_{12} = 0$, $\gamma \geq 0$, $l_{21} > 0$ and $l_{22} > 0$. Moreover, since the buoy $B2$ is on the surface, one has $y = l_{22}\cos(\beta)$ and $\alpha = -\beta$.

Consider first $y = 0$. Then, one has $\beta = 0$, $l_{21} = L$ and $l_{22} = l_2$, so the ROV is inside the area D1. This case is studied in Appendix J2.

Consider now $y > 0$.(15) becomes

$$l_{22}\cos(\beta) + h_{b2} = l_0 - l_1\cos(\gamma) - l_{21}\cos(\alpha) + l_{22}\cos(\beta)$$

$$0 = l_0 - h_{b2} - l_1\cos(\gamma) - l_{21}\cos(\beta) \quad (222)$$

From $y = l_{22}\cos(\beta) + h_{b2}$, one has

$$\cos(\beta) = \frac{y - h_{b2}}{l_{22}}. \quad (223)$$

Injecting (223) into (222), one gets

$$0 = l_0 - h_{b2} - l_1 \cos(\gamma) - (l_2 - l_{22}) \frac{y - h_{b2}}{l_{22}}$$
$$0 = l_{22}(l_0 - h_{b2} - l_1 \cos(\gamma)) - (l_2 - l_{22})(y - h_{b2})$$
$$L(y - h_{b2}) = l_{22}(l_0 - h_{b2} - l_1 \cos(\gamma) + (y - h_{b2}))$$
$$l_{22} = \frac{l_2 (y - h_{b2})}{l_0 - l_1 \cos(\gamma) + (y - 2h_{b2})} \quad (224)$$

and so $l_{21} = l_2 - \frac{l_2(y-h_{b2})}{l_0 - h_{b2} - l_1\cos(\gamma) + (y-h_{b2})}$. Remark since $l_0 \geq l_1 + \max([h_{b1}, h_{b2}])$, one has $\frac{(y-h_{b2})}{l_0 - l_1\cos(\gamma) + (y-2h_{b2})} \leq 1$, thus (224) guarantees that $0 \leq l_{22} \leq l_2$.

Let find the value of γ now. From (223), one has

$$\sin(\beta) = \sqrt{1 - \left(\frac{(y - h_{b2})}{l_{22}}\right)^2} \quad (225)$$

and injecting (224) inside (225), one obtains

$$\sin(\beta) = \sqrt{1 - \left(\frac{l_0 - l_1\cos(\gamma) + (y - 2h_{b2})}{l_2}\right)^2}. \quad (226)$$

By putting $X = \sin(\gamma)$, one gets

$$\sin(\beta) = \frac{1}{l_2}\sqrt{L^2 - \left(l_0 + y - 2h_{b2} - l_1\sqrt{1 - X^2}\right)^2}. \quad (227)$$

Using X and (227) inside (14), one gets

$$x = l_1 \sin(\gamma) + l_2 \sin(\beta)$$
$$x = l_1 X + \sqrt{l_2^2 - \left(l_0 + y - 2h_{b2} - l_1\sqrt{1 - X^2}\right)^2} \quad (228)$$

which can be rewritten such

$$(x - l_1 X)^2 = l_2^2 - \left(l_0 + y - 2h_{b2} - l_1\sqrt{1 - X^2}\right)^2$$
$$x^2 - 2l_1 xX + l_1^2 X^2 = l_2^2 - \left((l_0 + y - 2h_{b2})^2 + l_1^2 - l_1^2 X^2 - 2(l_0 + y - 2h_{b2}) l_1 \sqrt{1 - X^2}\right)$$

$$x^2 + (l_0 + y - 2h_{b2})^2 + l_1^2 - l_2^2 - 2l_1 xX = 2(l_0 + y - 2h_{b2}) l_1 \sqrt{1 - X^2}$$

$$\frac{x^2 + (l_0 + y - 2h_{b2})^2 + l_1^2 - l_2^2}{2(l_0 + y - 2h_{b2}) l_1} - \frac{x}{(l_0 + y - 2h_{b2})} X = \sqrt{1 - X^2} \quad (229)$$

Put $a_B = \frac{x^2 + (l_0+y-2h_{b2})^2 + l_1^2 - l_2^2}{2(l_0+y-2h_{b2})l_1}$ and $b_B = \frac{x}{l_0+y-2h_{b2}}$. A solution of (191) can be found studying

$$(a_B - b_B X)^2 = 1 - X^2 \quad (230)$$

Following the same steps developed for (192) in Section J1, one gets the following evaluation of γ such that

$$\sin(\gamma) = \begin{cases} X_{1B} & \text{if } (T_1 == True)\,\&\,(T_2 == False) \\ X_{2B} & \text{if } (T_1 == False)\,\&\,(T_2 == True) \\ \min([X_{1B},\, X_{1B}]) & \text{if } (T_1 == True)\,\&\,(T_2 == True) \end{cases} \quad (231)$$

with $T_1 = \left(a_B - b_B X_{1B} == \sqrt{1 - X_{1B}^2}\right)$, $T_2 = \left(a_B - b_B X_{2B} == \sqrt{1 - X_{2B}^2}\right)$ and

$$X_{1B} = \frac{a_B b_B - \sqrt{a_B^2 b_B^2 - (1 + b_B^2)(a_B^2 - 1)}}{(1 + b_B^2)} \quad (232)$$

$$X_{2B} = \frac{a_B b_B + \sqrt{a_B^2 b_B^2 - (1 + b_B^2)(a_B^2 - 1)}}{(1 + b_B^2)} \quad (233)$$

Finally, the evaluation of β is

$$\cos(\beta) = \frac{(y - h_{b2})}{l_{22}} = \frac{(y - 2h_{b2}) + l_0 - l_1\cos(\gamma)}{l_2}. \quad (234)$$

By considering the oriented angle convention

$$\beta = \text{sgn}(x)\,\text{acos}\left(\frac{(y - 2h_{b2}) + l_0 - l_1\cos(\gamma)}{l_2}\right). \quad (235)$$

K. Calculation of forces applied on the ROV

To choose the buoys in the capabilities of the ROV, this section exposes the strengths applied by the umbilical on the ROV. These ones depend of buoy choices, but also of the umbilical configuration, thus the area where the ROV is.

1) Strengths applied in areas A1 and B: Let $\vec{F}_{cable \to ROV}$ be the strength applied by the umbilical on the ROV and $\vec{T_3} = -\vec{F}_{cable \to ROV}$ where $\vec{T_3}$ is exposed in Section III-C. Then, by applied the FPS, one gets

$$\Sigma_{B2} \vec{F}.\vec{x} = 0$$
$$T_2 \sin(-\alpha) - T_3 \sin(\beta) = 0$$
$$T_3 \sin(\beta) = -T_2 \sin(\alpha). \quad (236)$$

Since $\alpha = -\beta$ in areas A1 and B, one has $T_3 = T_2$. Moreover, since $F_{cable \to ROV} = T_3$ and $F_{b2} = 2\cos(\beta) T_2$ from (132) in Appendix C, one gets

$$F_{cable \to ROV} = \frac{F_{b2}}{2\cos(\beta)}. \quad (237)$$

2) Strengths applied in areas A2: In area A2, one has from (137) and (142) shown in Appendix D

$$\begin{cases} T_3 \cos(\beta) & = F_{b2} + T_2 \cos(-\alpha) \\ F_{b1} & = 2\cos(\gamma) T_2 \end{cases} \quad (238)$$

Thus, since $\alpha = -\gamma$ in area A2, one gets

$$T_3 \cos(\beta) = F_{b2} + \frac{F_{b1}}{2\cos(\gamma)} \cos(-\alpha)$$
$$T_3 \cos(\beta) = F_{b2} + \frac{F_{b1}}{2}$$
$$T_3 = \frac{1}{\cos(\beta)}\left(F_{b2} + \frac{F_{b1}}{2}\right). \quad (239)$$

Since $F_{cable \to ROV} = T_3$, one has

$$F_{cable \to ROV} = \frac{1}{\cos(\beta)}\left(F_{b2} + \frac{F_{b1}}{2}\right). \quad (240)$$

3) Strengths in area D1: In area D1, the buoy $B1$ is in contact with the stop and $B2$ with the ROV. Then, by applied the FPS on $\vec{x}$ and $\vec{y}$, one gets from $\Sigma_{B2}\vec{F}.\vec{x}=0$

$$\begin{aligned} T_2\sin(-\alpha)+\vec{F}_{cable\to ROV}.\vec{x}&=0\\ \vec{F}_{cable\to ROV}.\vec{x}&=T_2\sin(\alpha), \end{aligned} \tag{241}$$

Moreover, one has from $\Sigma_{B2}\vec{F}.\vec{y}=0$

$$\begin{aligned} -T_2\cos(\alpha)+F_{b2}+\vec{F}_{cable\to ROV}.\vec{y}&=0\\ \vec{F}_{cable\to ROV}.\vec{y}&=T_2\cos(\alpha)-F_{b2}. \end{aligned} \tag{242}$$

From (241) and (242), one obtains

$$\begin{aligned} F_{cable\to ROV}&=\sqrt{\left(\vec{F}_{cable\to ROV}.\vec{x}\right)^2+\left(\vec{F}_{cable\to ROV}.\vec{y}\right)^2}\\ &=\sqrt{T_2^2+F_{b2}^2-2\cos(\alpha)T_2F_{b2}} \end{aligned} \tag{243}$$

with $F_{b1}\sin(\gamma)=T_2\sin(\gamma-\alpha)$, so

$$F_{cable\to ROV}=\sqrt{F_1^2\left(\frac{\sin(\gamma)}{\sin(\gamma-\alpha)}\right)^2+F_{b2}^2-2\cos(\alpha)\left(\frac{\sin(\gamma)}{\sin(\gamma-\alpha)}\right)F_{b1}F_{b2}} \tag{244}$$

4) Strengths in area D2: In area D2, the buoys $B1$ and $B2$ are is contact with the stop. Then, by applied the FPS on $\vec{x}$ and $\vec{y}$, one gets from $\Sigma_{B2}\vec{F}.\vec{y}=0$

$$\begin{aligned} (F_{b1}+F_{b2})-F_{cable\to ROV}\cos(\beta)&=0\\ F_{cable\to ROV}&=\frac{(F_{b1}+F_{b2})}{\cos(\beta)} \end{aligned} \tag{245}$$

The area D2 exists for $\beta\in\left]0,\frac{\pi}{2}\right[$, which solve division problem of (245).

5) Strengths in area D3: In area D3, the buoy $B2$ is in contact with the stop and $B1$ with the anchor. Then, by applied the FPS on $\vec{x}$ and $\vec{y}$, one gets from $\Sigma_{B2}\vec{F}.\vec{x}=0$

$$\begin{aligned} \sin(\beta)T_3-\sin(-\alpha)T_2&=0\\ T_2&=\frac{\sin(\beta)}{\sin(-\alpha)}T_3. \end{aligned} \tag{246}$$

Remind $F_{cable\to ROV}=T_3$. Injecting (246) inside $\Sigma_{B2}\vec{F}.\vec{y}=0$, one gets

$$\begin{aligned} -\cos(\beta)T_3+\cos(\alpha)T_2+F_{b2}&=0\\ \left(\frac{\sin(\beta)}{\tan(-\alpha)}-\cos(\beta)\right)T_3+F_{b2}&=0 \end{aligned}$$

$$F_{cable\to ROV}=\frac{F_{b2}}{\left(\frac{\sin(\beta)}{\tan(-\alpha)}-\cos(\beta)\right)}. \tag{247}$$

Remark $F_{cable\to ROV}=F_{b2}$ when $x=0$ so $\beta=0$ and $\alpha=\pi$, which is coherent because the cable l_2 is vertical and buoy $B2$ lifts directly the ROV.

L. Choice of umbilical parameters

1) Proof of (64) *:* The seafloor exploration is performed in area A2 to keep l_2 the most vertical possible, so let's choose l_1 and l_2 such $x_{\max}$ is inside area A2. First, the buoy $B2$ must not enter inside the exploration area to avoid collision with obstacle, thus take $l_2=\frac{y_{\text{floor}}-l_0}{\cos(\beta_{\max})}$. Let's now find l_1 such $\beta=\beta_{\max}$ at $x=x_{\max}$. Since $\gamma=-\alpha$ in area A2, using (23) for a couple (F_{b1},F_{b2}) such $F_{b2}>F_{b1}$, one can define

$$\begin{aligned} x_{\max}&=l_1\sin(\gamma)+l_2\sin(\beta_{\max})\\ x_{\max}&=l_1\sin\left(\operatorname{atan}\left(\frac{1}{\Lambda_{A2}}\tan(\beta_{\max})\right)\right)+l_2\sin(\beta_{\max})\\ x_{\max}-l_2\sin(\beta_{\max})&=l_1\frac{\frac{1}{\Lambda_{A2}}\tan(\beta)}{\sqrt{1+\left(\frac{1}{\Lambda_{A2}}\tan(\beta_{\max})\right)^2}}\\ l_1&=(x_{\max}-l_2\sin(\beta_{\max}))\sqrt{1+\left(\frac{1}{\tan(\beta_{\max})}\Lambda_{A2}\right)^2}. \end{aligned} \tag{248}$$

2) Proof of (62)*:* To have the longest umbilical possible with the surface constraints, the cable l_1+l_2 must start the lower possible, so take $l_0=y_{\max}$. Then, to guarantee the umbilical stays stretched when the ROV is inside the area $[y_{\min},y_{\max}]$, the maximum length possible for cable l_1+l_2 is $y_{\max}+y_{\min}$, *i.e.* to reach the surface from the anchor A and dive again to $y_{\min}$ with the buoy $B2$ on the surface. We choose to respect arbitrarily the ratio $\frac{F_{b1}}{F_{b2}}=\frac{l_2}{l_1}$, but take $l_2=l_1$ can be a valid choice. Thus, one has

$$l_2=\frac{F_{b1}}{F_{b2}}l_1. \tag{249}$$

To respect $l_1+l_2=y_{\max}+y_{\min}$, one gets

$$l_1=\frac{y_{\max}+y_{\min}}{\frac{F_{b1}}{F_{b2}}+1} \tag{250}$$

and $l_2=y_{\max}+y_{\min}-l_1$.